International Journal of Biological Macromolecules 321 (2025) 146209

Contents lists available at ScienceDirect

International Journal of Biological Macromolecules

journal homepage: www.elsevier.com/locate/ijbiomac

Fluorescence labeling-induced structural rearrangement of a monoclonal IgG revealed by biophysical experiments and simulations

Tímea Hajdu [a], István Rebenku [a], Tayde Gabriela Serrano Cano [a], Gábor Mocsár [a], Bálint Bécsi [b], Ferenc Erdődi [b], Peter Nagy [a,*]

[a] Department of Biophysics and Cell Biology, Faculty of Medicine, University of Debrecen, Debrecen, Hungary
[b] Department of Medical Chemistry, Faculty of Medicine, University of Debrecen, Debrecen, Hungary

ARTICLE INFO

Keywords:
Fluorescence labeling
IgG structure and dynamics
Hydrophobic effect

ABSTRACT

Although it is known that labeling antibodies with fluorescent dyes impairs their function, the underlying mechanism remains unclear. In this study, we show that multiple antibody functions decline in a strikingly similar way as the degree of labeling increases, suggesting that labeling induces a global structural change affecting the entire IgG molecule. Fluorescence anisotropy decay experiments revealed faster nanosecond-scale dynamics in labeled antibodies. FRET measurements showed that the Fc region moves closer to the hypervariable region upon labeling, further indicating major structural rearrangements. Molecular dynamics simulations confirmed that labeled antibodies adopt a more compact structure, bringing the Fc and Fab regions closer together. During simulations, the dye molecules gradually became less exposed to solvent, implicating the hydrophobic effect as a driver of structural collapse. The reduced antigen-binding affinity caused by labeling was partially restored by glycerol, likely due to its ability to weaken hydrophobic interactions. Together, these findings provide molecular-level insight into how fluorescent labeling disrupts antibody structure and function.

1. Introduction

The development of monoclonal antibodies in the 1970s and the widespread availability of organic fluorophores for their labeling ushered in a new era in cell biology. Although a large number of different fluorescent labeling approaches are at the disposal of researchers today, fluorophore-conjugated antibodies remain the cornerstone of labeling of antigens in cells and tissues due to the ease and sensitivity of fluorescence labeling. The most widely used approach for fluorescent labeling of antibodies is the coupling of dyes to ε-NH_2 groups of lysines resulting in a mixture of IgGs with different number of fluorophores randomly labeling available lysines [1,2]. While the fluorescent properties of antibody-conjugated dyes are largely retained in antibodies with a low degree of labeling (DOL, the mean number of fluorophores per antibody), quenching of fluorophores takes place in multiply-labeled antibodies [3]. This effect implies that dye-dye interactions, named self-quenching or concentration quenching, are primarily responsible for this phenomenon [3–6], which has been mainly attributed to static quenching processes [7]. Conversely, the functional properties of antibodies change much less upon fluorescence labeling due to the large difference in the molecular weight of the label and the labeled entity. However, the diminished affinity of fluorescently-labeled IgGs cannot be overlooked for antibodies heavily labeled by fluorophores [8–10], especially if their fluorescence intensity is to be evaluated quantitatively. In particular, it has been shown that the average DOL of the bound fraction of antibodies is lower than that of the stock solution due to preferential binding of low-DOL, and consequently higher affinity antibodies to antigens [7].

While the aforementioned phenomenon has been established and thoroughly investigated, its reason remains obscure. The epitope of an antigen is recognized by the paratope of an IgG comprising six complementarity-determining regions (CDR) with the heavy and light chains equally contributing three such hypervariable regions [11]. According to the classical modular structural model of antibodies, other antibody regions, especially the constant domains, are not involved in antigen binding, but they interact with other downstream effectors of the immune system, such as Fcγ receptors or the C1 complement complex [12]. However, recent immunological and structural data indicate that non-CDR regions of the variable domains, called framework regions, and even the constant domains of antibodies contribute to

* Corresponding author.
E-mail address: nagyp@med.unideb.hu (P. Nagy).

https://doi.org/10.1016/j.ijbiomac.2025.146209
Received 8 April 2025; Received in revised form 18 July 2025; Accepted 20 July 2025
Available online 22 July 2025

determining antigen specificity and affinity [13–15]. Several models have been put forward to account for these observations. Antigen binding has been proposed to be influenced by direct molecular interactions between residues proximal to the CDRs and the antigen, as well as by interdomain contacts between the VH1 and CH1 domains, or between the CH1 and CH2 domains [14–16]. According to another proposition, the overall secondary structure composition or the flexibility of antibodies are influenced by regions distant to the CDRs [17]. Low affinity antibodies are typically flexible and therefore promiscuous capable of binding a wider range of antigens. During antibody maturation, their flexibility significantly decreases accompanied by increased specificity and affinity, the latter being due to a reduction in the entropy penalty associated with binding [18–21].

In the current manuscript, we carried out a systematic investigation of the functions of different antibody domains in fluorescently labeled antibodies with different DOLs, and correlated the labeling-induced deterioration of these functions with each other, with the labeling-induced increased flexibility of antibodies and with a hydrophobic effect-dependent collapse of the structure of heavily labeled antibodies. We propose that the same dye-to-dye interactions responsible for reduced fluorescence also induce global structural alterations in the antibody, thereby diminishing its binding affinity.

2. Experimental

2.1. Cells

The SKBR-3 and THP-1 cell lines were obtained from the American Type Culture Collection (ATCC, Manassas, VA) and were grown according to their specifications. For microscopic experiments, cells were grown in 8-well chambers (Ibidi, catalog number: 80826) and for flow cytometry they were harvested by trypsinization. The JY human B lymphoblastoid cell line, kindly provided by Frances Brodsky (University of California, San Francisco), was grown in RPMI 1640 medium containing 10 % heat-inactivated fetal calf serum, 2 mM L-glutamine and antibiotics.

2.2. Antibodies and their fluorescence labeling

The mouse hybridoma producing the W6/32 ($IgG_{2a}(\kappa)$) monoclonal antibody specific for the heavy chain of MHC-I was kindly provided by Frances Brodsky (University of California, San Francisco). Trastuzumab (humanized $IgG_1(\kappa)$, RRID: AB_3112050) was purchased from Roche-Hungary (Budapest, Hungary), whereas cetuximab (humanized $IgG_1(\kappa)$, RRID: AB_3112048) was obtained from Merck Serono (Darmstadt, Germany). Fab fragments of W6/32 were generated with papain digestion using Pierce Fab Preparation Kit according to the manufacturer's instructions (catalog number 44985, ThermoFisher; for a brief description of the protocol, see the Supplementary material). Unlabeled, BP488-labeled, TAMRA-labeled and AlexaFluor647-labeled H98 (LLGPYELWELSH), a peptide recognized by trastuzumab, was synthesized by Pepscan [22]. Absorption and emission maxima of all different dyes used in the experiments are summarized in Supplementary Table 1.

The N-Hydroxysuccinimide esters of AlexaFluor546 and AlexaFluor647 dyes (Thermo Fisher Scientific, A20102 and A20106) were conjugated to purified monoclonal antibodies via primary amines according to the manufacturer's specifications (consult the Supplementary material for a brief description of the protocol). The dye-to-protein labeling ratio (degree of labeling, DOL) was determined for each labeled aliquot by spectrophotometry according to the manufacturer's instructions. A detailed description of the method is provided in the Supplementary material and in Supplementary Fig. 1.

Fc-specific labeling of trastuzumab was carried out using light-activated site-specific conjugation (LASIC) [23] according to the protocol provided by the company (AlphaThera). Briefly, oYo-Link Azide, specifically labeling the Fc part of antibodies, was mixed with a 1.5-fold molar excess of AlexaFluor488-DIBO-alkyne (C20020, ThermoFisher) or AlexaFluor594-DIBO-alkyne (C10407, ThermoFisher) and incubated at 37 °C for 2 h for orthogonal labeling of the azide group using click chemistry. The fluorophore-conjugated oYo-Link and trastuzumab were mixed in a molar ratio of 3:1 followed by photo-crosslinking for 2 h. UV illumination at 365 nm was generated using the LED PX device of AlphaThera. Unbound oYo-Link and unreacted DIBO-alkyne were separated from oYo-Link-conjugated trastuzumab using Bio-Spin 30 columns (7326231, Bio-Rad).

2.3. Functional tests of antibodies

Antibody binding to cell surface-expressed receptors was investigated by labeling 10^5 freshly harvested cells, washed twice in ice cold phosphate-buffered saline (PBS; pH 7.4), in 100 μL PBS supplemented with 1 mg/mL BSA on ice in the dark for 30 min. Unbound antibodies were removed by washing twice in PBS, and the resuspended samples were kept on ice until the measurement. For determining the saturation curve of fluorescently-tagged antibodies, a series of cell samples was incubated with different concentrations of the antibody, and their fluorescence intensity was recorded by flow cytometry followed by fitting a single-site binding equation to the data for determining the dissociation constant. In order to determine the affinity of an unlabeled antibody, 10^5 cells were incubated with a concentration series of the unlabeled antibody in the presence of a constant concentration of dye-conjugated antibody against the same epitope in 100 μL PBS supplemented with 1 mg/mL BSA on ice in the dark for 30 min. Unbound antibodies were removed by washing twice with PBS, and the resuspended samples were kept on ice until flow cytometric measurement. Data analysis was performed by assuming two ligands (labeled and unlabeled antibodies) competing for a single binding site. Details of the model are described in Supplementary materials.

For characterizing how efficiently antibodies bind to protein A or protein G, both binding to the CH2-CH3 interface [24–26], protein A- or protein G-coated microspheres (catalog numbers 553 and 554, Bangs Laboratories) were used. Binding of secondary antibodies to unlabeled and fluorescently-labeled W6/32 and trastuzumab was investigated using anti-mouse and anti-human Quantum Simply Cellular beads (for W6/32 and trastuzumab, respectively) (catalog numbers 815 and 816, Bangs Laboratories). The microspheres were incubated with the antibodies on ice for 30 min followed by washing twice in PBS and flow cytometry.

For measuring the binding of Fcγ receptors to the hinge-proximal region of the CH2 domain of IgGs [24,27], THP-1 cells were stimulated with 2000 U/mL interferon-γ (285-IF, R&D Systems) for 48 h to stimulate Fcγ receptor expression. Cells were washed twice in PBS and incubated with the investigated antibodies for 30 min on ice. In order to prevent potential binding of the anti-MHC-I W6/32 antibody by its antigen binding site, cells were preincubated with W6/32 Fab for 30 min before adding the W6/32 antibody to the cells. This procedure was not required for trastuzumab since its antigen, ErbB2, is not expressed by THP-1 cells. After the labeling, cells were washed twice in PBS and investigated by flow cytometry.

2.4. Flow cytometry

Flow cytometric measurements were carried out with a Novocyte 3000 RYB device equipped with three lasers (488/561/640 nm) (Agilent Technologies). AlexaFluor546 was excited with the 561-nm laser line and detected through a 586/20 nm bandpass filter after longer wavelengths were eliminated from the emitted light by a series of dichroic mirrors (735LP, 685LP, 650 LP, 600 LP, 572 LP). AlexaFluor647 was excited by the 640-nm laser line, and its emission was measured through a 660/20 nm bandpass filter after the emitted light passed through a series of dichroic mirrors (735 LP, 685 LP, 650 LP). Flow cytometric experiments were evaluated using FCS Express (De Novo Software,

Pasadena, CA). Live cells were identified on the forward scatter – side scatter (FSC/SSC) dot plot and the mean fluorescence intensity of the gated cells was calculated.

2.5. Nano-differential scanning fluorimetry

The thermal stability of labeled or unlabeled antibodies was investigated by nano-differential scanning fluorimetry using a Prometheus NT.48 instrument (NanoTemper Technologies). Samples were loaded into standard glass capillaries (NanoTemper Technologies, Munich, Germany), and placed onto the sample holder, then heated from 20 °C to 95 °C at a ramp rate of 1.0 °C/min. Three different concentrations (1.0, 2.0 and 3.0 μM) were used in duplicate for the unlabeled and labeled antibodies. The first derivative of the fluorescence ratio emitted at 350 nm and 330 nm (F350/F330) was calculated, after which Matlab was used to identify positive and negative peaks of sufficient prominence corresponding to the melting temperature (T_m).

2.6. Steady-state fluorescence anisotropy measurements

A Fluorolog-3 spectrofluorimeter (Horiba Jobin Yvon) was used for measuring steady-state anisotropy. AlexaFluor546 was excited at 550 nm and its fluorescence was detected at 590 nm. AlexaFluor647 was excited at 650 nm and its emission was recorded at 675 nm, while BP488 was excited at 490 nm and its emission was measured at 520 nm. The fluorescence anisotropy (r) was measured in the L-format according to the following formula [28]:

$$r = \frac{I_{VV} - G\,I_{VH}}{I_{VV} + 2\,G\,I_{VH}} \tag{1}$$

where I_{VV} and I_{VH} are the vertical and horizontal components, respectively, of the fluorescence excited by vertically polarized light, and G is a correction factor characterizing the different sensitivity of the detection system for vertically and horizontally polarized light:

$$G = \frac{I_{HV}}{I_{HH}} \tag{2}$$

where I_{HV} and I_{HH} are the vertical and horizontal components, respectively, of the fluorescence excited by horizontally polarized light. Binding of a small, fluorescent peptide, such as H98, to a large binder, such as trastuzumab, results in significant increase of its fluorescence anisotropy. This principle can be used for determining the dissociation constant of the trastuzumab-H98 complex, the details of which are summarized in the Supplementary material.

2.7. Time-dependent fluorescence anisotropy measurements

For time-dependent anisotropy measurements time-correlated single photon counting (TCSPC) was performed on an A1 confocal microscope (Nikon, Tokyo, Japan) equipped with a Plan-Apochromat 60× water immersion objective (NA = 1.27) and a time-correlated single-photon counting upgrade kit (PicoQuant). Pulsed excitation of AlexaFluor546 was achieved by a laser emitting ~1.5-ps pulses at 560 nm at a repetition rate of 20 MHz. Fluorescence emission was measured by two PMA hybrid 40 photon-counting photomultipliers (PicoQuant) recording the vertical and horizontal components between 570 and 620 nm. Both the emission of the fluorescent antibodies and the impulse response function were recorded for 10 × 10 s with a temporal resolution of 16 ps, and the curves were averaged. The vertical (I_{VV}) and horizontal (I_{VH}) intensity components can be described by the following equations:

$$I_{VV}(t) = I_{tot}(t)(1 + 2\,r(t)\,), I_{VH}(t) = I_{tot}(t)(1 - r(t)\,) \tag{3}$$

where $I_{tot}(t)$ is the time-dependent decay of fluorescence calculated from the previously determined fluorescence lifetimes, and $r(t)$ is the anisotropy decay calculated according to the following, two-component decay equation:

$$r(t) = r_0\left(f_1\, e^{-\frac{t}{\phi_1}} + (1 - f_1)\, e^{-\frac{t}{\phi_2}}\right) \tag{4}$$

where r_0 is the initial anisotropy at $t = 0$, ϕ_1 and ϕ_2 are the anisotropy decay time constants, and f_1 is the fraction of the anisotropy decaying with a time constant of ϕ_1. Both $I_{VV}(t)$ and $I_{VH}(t)$ were reconvolved with the impulse response function, and the experimentally determined decays of the vertical and horizontal intensities were globally fitted to this equation resulting in the ϕ_1 and ϕ_2 anisotropy decay time constants [29]. Analysis of time-dependent anisotropy decay was carried out with custom-written programs in Matlab.

2.8. Measurement of Förster resonance energy transfer (FRET)

Measurement of FRET efficiency is a versatile tool used for analyzing protein conformation and oligomerization. It usually involves a single donor-acceptor pair [30,31], but three-fluorophore systems can also be studied. For measuring the distance between the Fc part of an antibody and the antigen binding site, the tripleFRET approach was used according to a previously published method, which is briefly summarized in the Supplementary material in the section entitled "Triple-FRET measurements" [32]. The labeling scheme of antibodies is shown in Fig. 2. The triple-FRET system involves three dyes labeled by A, B and C with excitations wavelengths increasing in this order. Therefore, dye A undergoes FRET to B and C, and B is engaged in FRET with C. Each sample was recorded at three different excitation wavelengths, and fluorescence was integrated in three spectral regions corresponding to the emission ranges of the three dyes as shown in Fig. 2. The wavelengths were chosen to minimize spectral overspill between the different detection channels and direct excitation of the acceptor at the donor's wavelength. Spectral overspill was determined by measuring samples containing a single kind of fluorophore in the aforementioned detection channels, and determination of the FRET efficiency was performed as described previously [32]. Distances were calculated from the FRET efficiencies according to the following equations:

$$R_{AB} = R_{0,AB}\left(\frac{1 - E_{AB} - E_{AC}}{E_{AB}}\right)^{\frac{1}{6}}, R_{AC} = R_{0,AC}\left(\frac{1 - E_{AB} - E_{AC}}{E_{AC}}\right)^{\frac{1}{6}}, R_{BC} = R_{0,BC}\left(\frac{1 - E_{BC}}{E_{BC}}\right)^{1/6} \tag{5}$$

where E designates the FRET efficiency between the dyes specified in the subscript, R stands for the distance between the dyes specified in the subscript, and R_0 is the Förster radius corresponding to the dyes specified in the subscript [33].

2.9. Molecular dynamics simulations and their analysis

The full-length, glycosylated structure of trastuzumab was obtained from a previous publication [34]. Trastuzumab is a humanized monoclonal antibody of the isotype $IgG_1(\kappa)$ having two light and two heavy chains corresponding to the following residue numbers in the structure: chain A (heavy, residues 1–450), chain B (light, residues 451–664), chain C (heavy, residues 665–1114), chain D (light, residues 1115–1328). The 2D structure of AlexaFluor546 was downloaded from PubChem (PubChem ID: 25164103). The 2D structure of AlexaFluor647 NHS ester was also downloaded from PubChem (PubChem ID: 167996453) and was converted to the free acid in Desmond (D. E. Shaw Research), followed by a 50-ns simulation in TIP3P water to obtain the 3D structures of both dyes. These free dyes were esterified to the following lysine residues evenly distributed along the amino acid sequence: Lys249, Lys251, Lys329, Lys343 – heavy chain A; Lys492, Lys495, Lys553, Lys619 – light chain B; Lys913, Lys1005 – heavy chain

C; Lys1156, Lys1217 – light chain D. The system was solvated in an orthorhombic box of TIP3P water molecules with a 25 Å boundary. All MD simulations were preceded by two stages of minimization (restrained and unrestrained) followed by four stages of MD runs with gradually diminishing restraints. Production MD simulations were carried out using the OPLS force field and the NPT ensemble class at 300 K and 1.01325 bar. The solvent accessible surface area was determined in VMD (Theoretical and Computational Biophysics group at the Beckman Institute, University of Illinois at Urbana-Champaign, IL) by extending the radius of each atom by 1.4 Å to find the points on the sphere that are exposed to solvent [35]. The number of water molecules around the fluorescent dyes was also determined in VMD by selecting the dye molecules and counting the number of TIP3P water molecules within a radius of 3 Å around them. The number of hydrogen bonds, the root mean square fluctuation and the root mean square deviation of trastuzumab were determined in Desmond in the "Interactions" panel and using the "Simulation Interactions Diagram" tool. Secondary structure assignment was performed using the STRIDE algorithm in VMD [36].

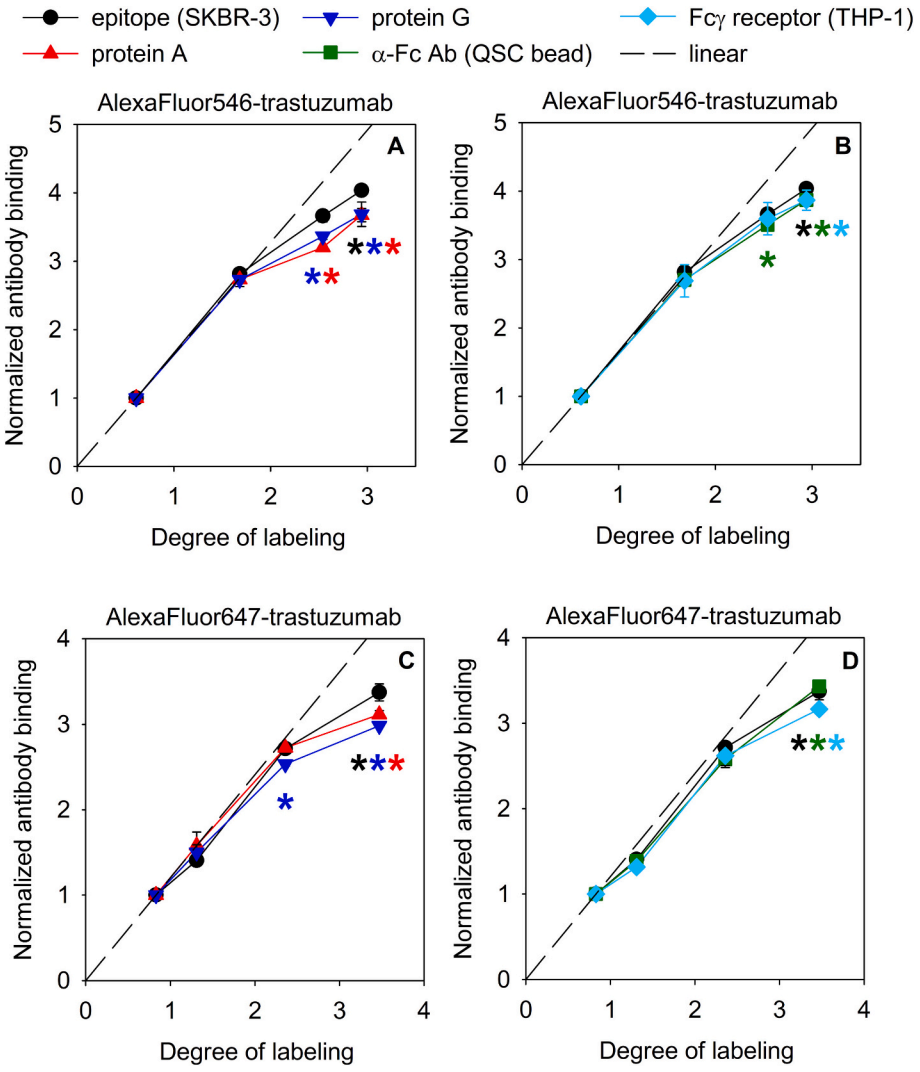

Fig. 1. Testing the functional properties of different domains of trastuzumab as a function of the degree of labeling. Trastuzumab was labeled either with AlexaFluor546 (A,B) or AlexaFluor647 (C,D) fluorophores. Antibody batches with four different degrees of labeling were generated, and their degree of labeling was determined by spectrophotometry. The epitope binding capability of the antibodies was tested by measuring their binding to SKBR-3 cells expressing ErbB2, the antigen recognized by trastuzumab (●). Their potential to bind to protein G or protein A was estimated by measuring their binding to protein G- (▼) or protein A-coated (▲) beads, respectively. The binding of W6/32 to Fcγ receptors was tested by measuring their binding to THP-1 cells expressing Fcγ receptors (◆). The ability of trastuzumab to be recognized by anti-human Fc receptor antibodies was tested by measuring its binding to anti-Fc antibody-coated QSC beads (■). In order to circumvent overcrowding of figures, the binding of trastuzumab to SKBR-3 cells (●) is displayed in both the left- and right-hand figures, while binding to protein A and protein G (▲, ▼) is only shown in the left-hand figures, and binding to Fcγ receptors and to anti-Fcγ receptor antibodies (◆, ■) is only shown in the right-hand figures. Binding was measured by flow cytometry, and mean fluorescence intensities of flow cytometric histograms were normalized to the degree of labeling of the antibody batch with the lowest degree of labeling. This way of determining "normalized antibody binding", plotted on the vertical axis, results in a value of 1 for the antibody with the lowest degree of labeling. The dashed lines show how the normalized antibody binding would change if it were a linear function of the degree of labeling. The graphs show the mean of three independent experiments (±the standard error of the mean). The asterisks indicate that the normalized antibody binding is significantly different from the linear expectation (the dashed line) that would be observed if the fluorescence intensity of the bound antibody fraction were proportional to the degree of labeling. One-sample *t*-tests were carried out, and a significant difference was concluded for $p < 0.05$ adjusted for multiple comparisons according to Bonferroni. The color of the asterisks matches the color of the symbols.

3. Results

3.1. Deterioration of several antibody functions depends identically on the degree of labeling

Although it is acknowledged in the literature that the affinity of an antibody to its epitope is impaired by fluorescence labeling [7–10], it is neither known whether other antibody functions are affected in a similar way, nor is the mechanism behind this phenomenon certain. To address the former question, we selected several known interaction partners of IgGs and tested how their binding depends on the degree of labeling. Protein A and protein G binding is mediated by the junction of the CH2 and CH3 domains [24–26], whereas binding to Fcγ receptors takes place through the hinge-proximal region of the CH2 domain [24,27]. The overall structural intactness of the Fc portion was tested by the ability of anti-Fcγ antibodies to bind to the unlabeled and labeled antibodies. Throughout the experiments, we used two different kinds of antibodies, a mouse monoclonal antibody, W6/32 ($IgG_{2a}(\kappa)$), raised against human MHC-I, and a humanized, mouse monoclonal antibody, trastuzumab ($IgG_1(\kappa)$), against human ErbB2. The antibodies were labeled with AlexaFluor546 or AlexaFluor647 fluorescent dyes to achieve a range of different degrees of labeling followed by measuring the binding of these antibodies to their epitope, protein A, protein G, Fcγ receptors or to anti-Fc antibodies. All of these five antibody functions revealed remarkably similar dependence on the degree of labeling for both antibodies and for both dyes (Fig. 1, Suppl. Fig. 2). Since we considered epitope binding the most important antibody function from the standpoint of cell biological applications, we quantitatively determined the dissociation constant characterizing antibody binding to cell surface-exposed antigens revealing labeling-induced decreased affinity in a quantitative way (Suppl. Fig. 3). Consistent with our earlier observations, AlexaFluor647 had a greater detrimental effect on antibody affinity than AlexaFluor546 [7]. Fab fragments prepared from one of the tested IgGs, W6/32, also exhibited gradually diminishing affinity as a function of the degree of labeling (Suppl. Fig. 3; preparation of Fab fragments from trastuzumab was unsuccessful). If fluorescence labeling did not affect either the fluorescence properties of dyes or the affinity of antibodies, the fluorescence intensity of antibodies bound to their binding partners would increase in a linear fashion with the degree of labeling. As quantitatively modeled in a previous publication [7], deviation from this linear tendency is a complex function of how antibody affinity and the fluorescence quantum efficiency of the dyes change as a function of the degree of labeling. Multiple studies have shown that fluorescence labeling reduces both the fluorescence quantum yield of dyes and the antigen affinity of antibodies [7–10]. The observation that all antibody functions decline in proportion to antigen affinity as the degree of labeling increases suggests that fluorescence labeling affects all functions to a similar extent as epitope binding. Based on this reasoning, we hypothesized that fluorescence labeling induces a global structural or dynamic alteration in antibodies, leading to significant and comparable changes in functions associated with different antibody domains (see Discussion for a deeper consideration of this assumption).

3.2. Fluorescence labeling-dependent alterations in the structural properties of antibodies

Having obtained indirect proof for fluorescence labeling-induced global alterations in the structural properties of antibodies, we applied different experimental approaches to find evidence for these structural changes. Since most of these measurements required incubation of antibodies with a soluble antigen, a peptide, H98, isolated from a phage display library was used as an epitope recognized by trastuzumab [22]. We used two techniques to characterize the binding affinity of H98: (1) fluorescence anisotropy measurements to characterize the binding of fluorescently labeled H98 to trastuzumab in solution; and (2) competitive binding experiments in which both unlabeled and fluorescently labeled H98 inhibited the binding of trastuzumab to cell surface-expressed ErbB2. These experiments established that H98 binds to trastuzumab with a dissociation constant in the micromolar range (Suppl. Fig. 4). Furthermore, we showed the lack of nonspecific binding of H98 to cetuximab, an isotype-matched humanized anti-EGFR antibody (Suppl. Fig. 5). Next, we applied Förster resonance energy transfer (FRET) to measure the distance between the Fc part and the epitope binding region of trastuzumab in order to gain insight into the size of the antibody molecule before and after fluorescence labeling. To this end, we used light-activated site-specific conjugation (LASIC) in which a protein G-derived polypeptide (oYo), labeled by click-chemistry with a fluorescent dye serving as a donor in FRET experiments, has been photocrosslinked to the Fc part of trastuzumab [23]. Furthermore, we used one of the fluorescent H98 antigenic peptides binding to the hypervariable region of trastuzumab as a FRET acceptor. The labeling scheme is summarized in Fig. 2. Since we wanted to perform the FRET experiments with both unlabeled and fluorescently labeled trastuzumab, the presence of the third kind of dye on the labeled antibodies resulted in a triple-FRET system in which energy is transferred between three fluorescent dyes [32]. After compensating for spectral spillover and confounding FRET, the FRET efficiency between the dyes labeling the Fc and hypervariable regions of trastuzumab could be calculated. The FRET values and the distances calculated from them revealed that the separation between the Fc and hypervariable regions of trastuzumab with a high degree of labeling is significantly smaller than in unlabeled trastuzumab or trastuzumab with a low degree of labeling (Fig. 3). The distance of ~10 nm for the separation between the Fc part (oYo-binding site) and the epitope binding region is in accordance with the molecular dimensions of IgGs [34]. Although inspection of the emission spectra, from which the FRET efficiencies were determined, does not allow accurate evaluation of the FRET measurements due to the large number of spectral overspills, there are certain qualitative signs implying that FRET indeed takes place between the dyes labeling the Fc and the hypervariable regions of the antibody (Suppl. Fig. 6). Although anisotropy experiments shown in Suppl. Fig. 5 revealed no unspecific binding of the antigenic H98 peptide to trastuzumab, we confirmed the specific binding of H98 to trastuzumab in the FRET experiments by showing that FRET between the Fc and hypervariable regions was essentially eliminated by inhibiting the binding of acceptor-conjugated H98 by a 10-fold molar excess of unlabeled H98 (Suppl. Fig. 7).

The FRET measurements revealed the equilibrium structure of the antigen-bound antibody. Since we were interested in any potential labeling-induced change in the antigen binding process, we next interrogated its energetic landscape by applying the van't Hoff equation to temperature-dependent binding measurements. Binding of fluorescently labeled H98 to unlabeled and fluorescently labeled trastuzumab was measured by incubating a constant concentration (3 μM) of fluorescent H98 with different concentrations of trastuzumab at four different temperatures (24 °C, 29 °C, 34 °C, 39 °C) followed by measuring the fluorescence anisotropy of H98 and finding the dissociation constant of the H98-trastuzumab complex at the four different temperatures by fitting. The temperature-dependent change of the dissociation constant allowed us to determine the standard enthalpy and entropy of binding (Fig. 4A). The standard enthalpy and entropy of binding for the complex of H98 and unlabeled trastuzumab revealed that the binding reaction is enthalpically favored, but entropically unfavorable under standard conditions (Table 1). Fluorescence labeling increased both the standard enthalpy and entropy of binding implying that the formation of the antibody-antigen complex becomes enthalpically less favored and entropically less punished after fluorescence labeling of the antibody (Table 1).

Since glycerol has been known for decades to stabilize proteins [37,38], we argued that it may have a beneficial effect on the antigen binding affinity of fluorescently labeled trastuzumab. Therefore, we determined the dissociation constant of H98 in complex with unlabeled and fluorescently labeled trastuzumab in purely aqueous medium and in

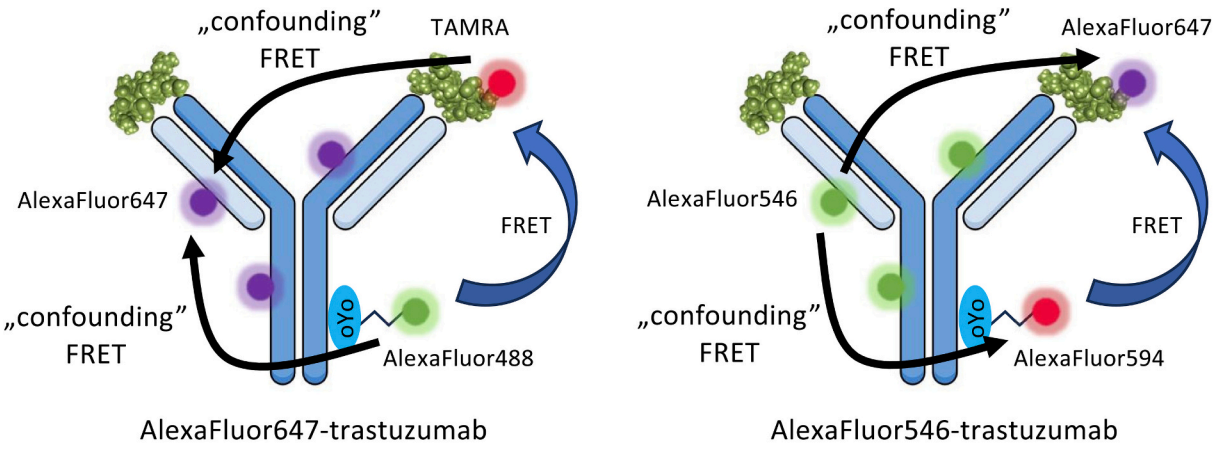

Symbol	Description	Excitation [nm]	Emission [nm]
I_{AA}	A488	488	510-550
I_{AB}	A488→TAMRA	488	555-650
I_{AC}	A488→A647	488	660-750
I_{BB}	TAMRA	543	555-650
I_{BC}	TAMRA→A647	543	660-750
I_{CC}	A647	647	660-750

Symbol	Description	Excitation [nm]	Emission [nm]
I_{AA}	A546	561	570-590
I_{AB}	A546→A594	561	591-660
I_{AC}	A546→A647	561	661-750
I_{BB}	A594	580	591-660
I_{BC}	A594→A647	580	661-750
I_{CC}	A647	650	661-750

Fig. 2. Scheme of triple-FRET measurements with fluorescently-labeled antibodies. The Fc part of AlexaFluor647- and AlexaFluor546-tagged trastuzumab was site-specifically labeled by oYo-link that was conjugated with AlexaFluor488 or AlexaFluor594 using click-chemistry. FRET between the dye on the oYo-link and the fluorescently labeled antigenic peptide was measured (blue arrows), but due to the presence of the fluorophores on the antibody, two more FRET processes, labeled by the black arrows, also had to be taken into consideration. These "confounding" FRET processes arise due to spectral overspill, i.e., even though only the dye attached to the oYo-Link is intended to be excited, it is inevitable to excite the other fluorophores in the antibody as well. To account for such spectral overspills, the FRET measurements had to be carried out in six channels. The table under the antibodies shows the detection wavelengths of these six measurements corresponding to the directly-excited and the FRET-sensitized emissions (the latter containing an arrow symbol in their description). In the "symbol" column letters A, B and C designate the dyes in the order of their excitation wavelengths (A, B and C correspond to AlexaFluor488 (A488), TAMRA and AlexaFluor647 (A647) in the table on the left, while they designate AlexaFluor546 (A546), AlexaFluor594 (A594) and AlexaFluor647 (A647) in the table on the right). The first and second letters in the indices of symbols correspond to the excited dye and the dye whose emission was measured, e.g., I_{AC} means that excitation was carried out at the excitation wavelength of dye A, and the fluorescence was recorded in the emission wavelength range of dye C.

55 % (*v*/v) glycerol. Data of a representative measurement is shown in Suppl. Fig. 8. For both the unlabeled and fluorescently labeled trastuzumabs, glycerol decreased the affinity of the antibody to the antigen (Suppl. Table 2). Glycerol is known to have variable effects on the stability of an antigen-antibody complex [39], and the effect observed in the experiments is likely attributable to the significantly reduced collisional frequency in the high viscosity medium. The data also shows that fluorescence labeling reduced the stability of the antigen-antibody complex in accordance with data presented in Suppl. Fig. 3. Even more importantly, the fluorescence labeling-induced reduction in the affinity of trastuzumab observed in glycerol was significantly less than in purely aqueous medium implying that glycerol partially inhibited the detrimental effect of fluorescence labeling on antibody affinity (Fig. 4B).

The results obtained with glycerol, an agent known to stabilize protein structure, suggest that fluorescence labeling may alter the stability of antibodies. In order to test whether these changes are manifested in an altered melting temperature, we performed nano-differential scanning fluorometry experiments revealing two distinct melting temperatures for unlabeled trastuzumab corresponding to denaturation of the Fc and Fab domains, and one resolved peak for unlabeled W6/32 (Suppl. Fig. 9). The presence of a variable number of peaks in the nanoDSF spectra of antibodies is well-documented [40]. The derivative of the ratio of tryptophan fluorescence emitted at 350 nm and 330 nm was positive for trastuzumab and negative for W6/32, a phenomenon that can be attributed to the different water exposure of tryptophan residues in the native, folded proteins [41]. Labeling with either AlexaFluor546 or AlexaFluor647 had no effect on the melting temperatures of either trastuzumab or W6/32 antibodies suggesting that the presence of fluorescent dyes does not alter the thermal stability of the antibody (Suppl. Fig. 9).

3.3. Fluorescence labeling alters the dynamics of antibodies revealed by fluorescence anisotropy measurements

In the previous sections, the equilibrium structure of unlabeled and fluorescently labeled antibodies was interrogated obscuring structural fluctuations known to be fundamental in the formation and rearrangement of the ligand binding site. It has been pointed out specifically for antibodies that their affinity is closely related to their dynamic flexibility [18–21]. Therefore, we applied time-dependent fluorescence anisotropy decay for studying the molecular motions of antibodies in the nanosecond to tens-of-nanoseconds time range. To this end, we labeled trastuzumab and W6/32 antibodies with AlexaFluor546 to achieve three different degrees of labeling and measured the decay of the fluorescence anisotropy of AlexaFluor546. The fluorescence lifetime of AlexaFluor647 is ~1 ns making it unlikely that motions on a timescale of

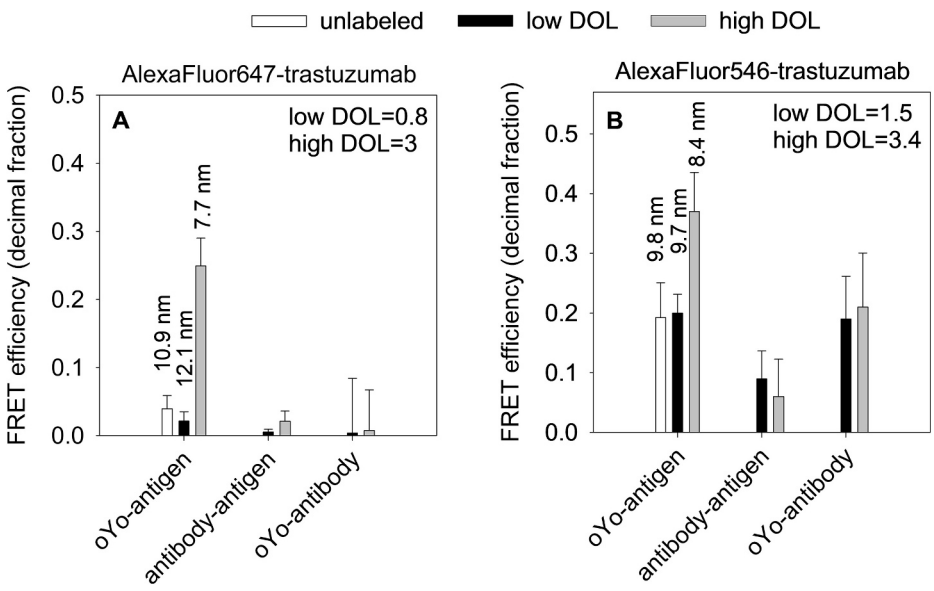

Fig. 3. Triple-FRET measurements to reveal the distance between the Fc and hypervariable regions of trastuzumab. Trastuzumab was labeled by either AlexaFluor647 (A) or AlexaFluor546 (B) to achieve two different degrees of labeling determined by spectrophotometry. The Fc part of AlexaFluor647-labeled trastuzumab was further labeled by AlexaFluor488-oYo-Link, and this double-labeled antibody was complexed with TAMRA-conjugated H98 peptide as an antigen. The Fc part of AlexaFluor546-labeled trastuzumab was crosslinked to AlexaFluor594-oYo-Link, and AlexaFluor647-H98 antigenic peptide was mixed with this double-labeled antibody. The labeling scheme is summarized in Fig. 2. Triple-FRET measurements were carried out by fluorometry, and the mean FRET efficiencies (±standard error of the mean calculated from three independent measurements) between the three labeled parts of the antibodies were calculated. "oYo" is the label on the Fc portion, "antigen" stands for the H98 peptide, and "antibody" represents the fluorescent label that is conjugated to the antibodies using conventional N-hydroxysuccinimide ester chemistry. The distances corresponding to the most important distance between the Fc part and the hypervariable region ("oYo-antigen") are displayed above the corresponding bars.

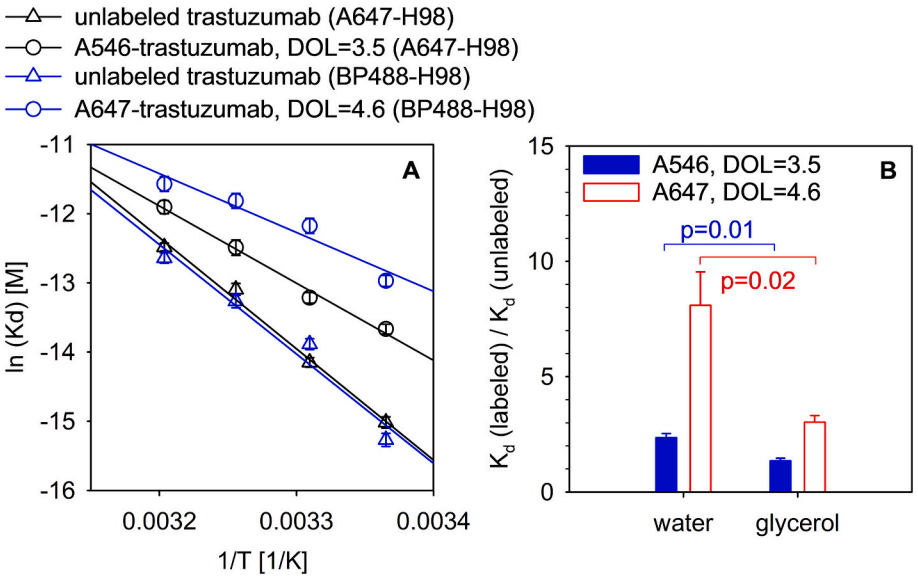

Fig. 4. Thermodynamic analysis of the antigen binding affinity of unlabeled and fluorescently-labeled trastuzumab. Trastuzumab was labeled with AlexaFluor546 or AlexaFluor647 (abbreviated A546 and A647 in the figure), and its degree of labeling (DOL) was determined by spectrophotometry. The affinity of the AlexaFluor546-labeled antibody to the H98 antigenic peptide was determined by measuring the fluorescence anisotropy of AlexaFluor647-H98, while the dissociation constant of the AlexaFluor647-conjugated antibody was analyzed by measuring the anisotropy of BP488-H98. As a reference, the binding of unlabeled trastuzumab was determined to both kinds of fluorescently-labeled H98 peptides. (A) Measuring the dissociation constant as a function of temperature and plotting the logarithm of K_d as a function of $1/T$ allowed us to determine the standard enthalpy and entropy of binding. The standard enthalpy and entropy of binding are shown in Table 1. The graph corresponds to the dissociation process, but the table displays the constants corresponding to the association (binding) reactions. (B) The binding affinity of unlabeled, AlexaFluor546- and AlexaFluor647-conjugated trastuzumab to H98 was determined at room temperature both in water and 55 % (v/v) glycerol, and the fold-increase in the dissociation constant caused by fluorescence labeling (±standard error of the mean) was calculated (B).

nanoseconds to tens of nanoseconds can be measured using this dye. Two decay components were revealed in the analysis of the anisotropy curves of both antibodies (Fig. 5). The fast component characterized by a time constant of 1–2 ns most likely corresponds to molecular motions of the dyes and its photophysical processes (see Discussion for further details). The slow component characterized by a time constant of 10–40

Table 1
The standard enthalpy and entropy of binding of the trastuzumab-H98 complex determined from the data presented in Fig. 4. The values in parentheses display the 95 % confidence interval of the parameters.

Antigen	Antibody	Standard enthalpy of binding (ΔH_0, kJ/mol)	Standard entropy of binding (ΔS_0, J/(K mol))
AlexaFluor647-H98	Unlabeled trastuzumab	−133.7 (−169.8, −97.5)	−325 (−444, −206)
	AlexaFluor546-trastuzumab (DOL = 3.5)	−92.8 (−119.4, −66.2)	−198 (−285, −111)
BP488-H98	Unlabeled trastuzumab	−133.4 (−213.8, −49.1)	−317.1 (−587.2, −162)
	AlexaFluor647-trastuzumab (DOL = 4.6)	−70.7 (−127.7, −23.7)	−131.4 (−218, −59)

ns likely corresponds to the flexibility and twisting motions of the antibody [42]. Comparing the anisotropy decays of both antibodies revealed that the slow component was faster in antibodies with a high degree of labeling implying that molecular motions in this time domain are accelerated by fluorescence labeling. Although the time scale of these molecular motions is substantially longer than the fluorescence lifetime of AlexaFluor546, the differences between the decay curves allowed reliable discrimination between the antibodies with different degrees of labeling (Suppl. Fig. 10).

Increasing the degree of labeling reduces the average distance between dyes in a single antibody enhancing the probability of homo-FRET, which is known to accelerate anisotropy decay. Although the characteristic anisotropy decay time constant associated with homo-FRET is expected to be in the nanosecond time range [43], we wanted to ascertain that the accelerated anisotropy decay of antibodies with a high degree of labeling is not due to this phenomenon. To this end, we compared the anisotropy decay of three different antibody samples. One of them was labeled to a low degree of labeling with AlexaFluor546, the second one was labeled with AlexaFluor546 to achieve high degree of labeling, while the third one was labeled with a mixture of AlexaFluor546 and AlexaFluor488. The total degree of labeling of this antibody sample was close to the other one with a high degree of labeling with only AlexaFluor546. However, the fact that the number of AlexaFluor546 molecules on this dual-labeled antibody was lower than in the one labeled to a high degree with only AlexaFluor546 reduces the probability of homo-FRET taking place between AlexaFluor546 dyes. The fact that the slow anisotropy decay component of the dual-labeled antibody and the one labeled with many AlexaFluor546 molecules are similar implies that the labeling-induced accelerated anisotropy decay in the 10–40 ns time range is at least partially due to faster molecular motions of highly labeled antibodies, and not to homo-FRET (Suppl. Fig. 11).

While previous fluorescence anisotropy decay studies of IgGs attributed the decay components mainly to motions of the Fab and Fc fragment relative to each other [44], it was argued in more recent investigations that intradomain flexibility and intradomain elbow motions significantly contribute to both the dynamics of antibodies and the consequent anisotropy decay [42,45,46]. Therefore, we prepared Fab fragments from the W6/32 antibody and labeled them with AlexaFluor546 to achieve three different degrees of labeling followed by fluorescence anisotropy decay experiments. Unfortunately, attempts to

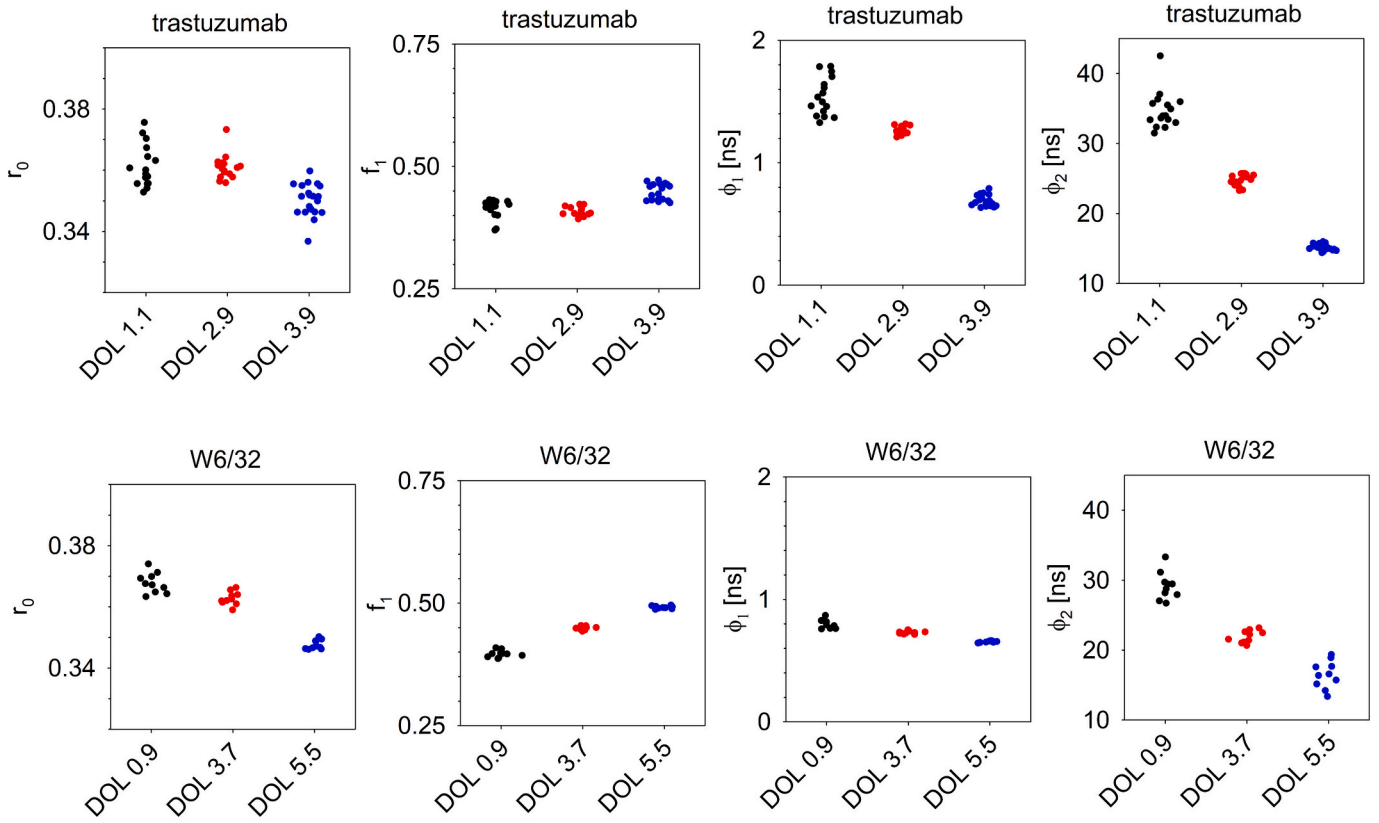

Fig. 5. Analysis of the fluorescence anisotropy decay of AlexaFluor546-labeled trastuzumab and W6/32. Trastuzumab and W6/32 antibodies were labeled by AlexaFluor546 (A546), and their degrees of labeling (DOL) were determined by spectrophotometry. Time-dependent fluorescence anisotropy decay curves were recorded by time-correlated single photon counting followed by analysis of the anisotropy decay parameters using a reconvolution approach. The maximum anisotropy (r_0), the fraction of the first anisotropy decay component (f_1) and the anisotropy decay time constants of the first and second components (φ_1, φ_2) of individual measurements are shown in the figure.

prepare Fab fragments from trastuzumab were unsuccessful. The fast component of the anisotropy decay of Fabs was faster than in IgGs. Even more remarkably, the slow component characterized by time constants of 20–30 ns was accelerated in Fabs with a high degree of labeling (Suppl. Fig. 12). These results imply that the presence of multiple dyes results in faster intradomain flexible or elbow motions of Fab fragments.

3.4. Molecular dynamics simulations suggest a hydrophobic effect-mediated collapse of the structure of labeled antibodies

Evidence presented in the previous sections strongly suggests that fluorescence labeling leads to profound changes in antibody structure and dynamics. In order to get direct insight into the structural alterations themselves, we performed molecular dynamics (MD) simulations with unlabeled and fluorescently labeled trastuzumab. The full-length structure of trastuzumab has been constructed previously from the crystal structure of the Fab domain of trastuzumab and the G2-glycosylated Fc domain of a closely related antibody that was mutated in silico to make it identical to the Fc domain of trastuzumab [34]. This structure has been validated by comparing MD simulations to results of hydrodynamic modeling. We labeled this full-length trastuzumab structure with AlexaFluor546 or AlexaFluor647 molecules in silico. The lysines labeled for the simulations were selected so that they were approximately homogeneously distributed among the possible labelable lysines. We chose a high in-silico degree of labeling to amplify dye-dye and dye-protein interactions, which allowed us to characterize mechanisms that would otherwise require much longer simulation times. Furthermore, such highly labeled antibodies are also present in antibody samples with a lower average degree of labeling, and they disproportionately affect the photophysics of dyes and the biological properties of the antibodies. We performed four runs of 100-ns MD simulations to compare the structure and dynamics of unlabeled and labeled antibodies. The root mean square deviation (RMSD) of the unlabeled structure in the current simulations plateaued at ~15 Å in perfect agreement with literature data [34] (Suppl. Fig. 13). This observation along with the similar RMSD values of the fluorescently labeled antibodies argues that the simulated structures were stable. The unlabeled antibody exhibited significant motion of the Fab and Fc fragments relative to each other with the overall structure of the individual domains being preserved. Furthermore, while the Fab and Fc fragments occasionally moved closer to each other, this juxtaposition was only temporary (Fig. 6, Suppl. Movie 1). In striking contrast, the domains of the fluorescently labeled antibodies remained in proximity after their initial contact with each other resulting in a collapse of the domains onto each other (Fig. 6, Suppl. Movies 2, 3). These observations are in qualitative agreement with the FRET experiments showing that the Fc and Fab domains are closer to each other in labeled antibodies (Fig. 3). We determined whether the distance between the Fc and Fab domains in the MD simulations is in agreement with the FRET results by calculating the average distance between Thr58 and Asn437 in the heavy chain. Thr58 in the heavy chain is in the epitope binding region of trastuzumab [47]. Asn437 of the heavy chain is within the region binding to protein G from which the Fc-specific oYo-Link was engineered [23,26]. Therefore, the distance between Thr58 and Asn437 corresponds to the approximate separation between the fluorescently labeled antigen and the oYo-link conjugated to the Fc part. The mean of four distances (Thr58(A)-Asn437(A), Thr58(A)-Asn437(C), Thr58(C)-Asn437(C), Thr58(C)-Asn437(A), the letter in parentheses specifies the polypeptide chain) was calculated revealing that the separation between the approximate position of the oYo-Link and the epitope binding regions was significantly larger at the end of the trajectories in unlabeled trastuzumab than in the two fluorescently labeled antibodies (Fig. 7A). These distances are substantially larger than the experimentally determined ones in Fig. 3 since the amino acid residue in the Fc part is obviously farther away from the epitope binding region of the Fab on the opposite side of the molecule, and this distance also contributes to the mean. Using the aforementioned four individual distances between the approximate positions of the oYo-Link and the epitope binding regions in the last 30 ns of the stimulation, we calculated the expected FRET efficiencies (Suppl. Fig. 14), which were consistent with the experimental results in Fig. 3. The lack of exact correspondence between the measured and the calculated FRET values can be attributed to the fact that (i) we were only able to determine the position of the epitope approximately in the MD simulations; (ii) the antigen binding site is probably closer to the dye on the oYo-Link than to Asn437 in the heavy chain due to the size of the oYo-Link itself; and (iii) the relative orientation of the donor and the acceptor and whether dynamic averaging applies are unknown. However, the general agreement between the simulated and the experimentally determined FRET values provides support to the model in which the increased FRET efficiency between the Fc and antigen binding regions of antibodies with a high degree of labeling is caused by the collapse of the antibody structure revealed by the MD simulations. Furthermore, we can conclude that fluorescence labeling results in a collapse of the antibody structure by making interdomain contacts more lasting than in unlabeled antibodies.

In order to find the reason for the aforementioned structural alterations in labeled antibodies, we calculated the solvent accessible surface area (SASA) of the dyes in both the AlexaFluor546- and AlexaFluor647-conjugated antibodies. SASA decreased monotonously as a function of simulation time, and it was reduced by 1000–1500 $Å^2$ from the first 10 ns to the last 10 ns of the simulation (Fig. 8AB). SASA of the whole antibody structure did not change significantly during the simulations (data not shown). In accordance with these observations, the number of water molecules in contact with the dyes decreased as a function of simulation time (Fig. 8CD). Both the decreased SASA and the reduced number of water molecules in contact with the dyes point at a hydrophobic effect-mediated process. We also determined the number of hydrogen bonds in the antibodies. While it stayed constant for unlabeled antibodies, it increased in both AlexaFluor546- and AlexaFluor647-conjugated antibodies (Fig. 8EF). Although the radius of gyration and the volume of the bounding box of the Fc and Fab parts did not change during simulations (data not shown), the increase in the number of hydrogen bonds during simulations implies that the structure of labeled antibodies became more compact.

The increased number of hydrogen bonds in the structure of fluorescent antibodies suggested that subtle alterations took place in the non-covalent bonds in antibodies. Although the nanoDSF measurements implied that these changes are unlikely to be significant, we wanted to check if there was any change in the secondary structure composition of the simulated antibodies. In agreement with available structural information, the overwhelming majority of amino acid residues reside in β-sheets [48] (extended configuration and turns connecting them in Suppl. Fig. 15). Fluorescent labeling left this overall pattern unchanged, indicating that the antibodies' secondary structure remained intact.

Both the anisotropy measurements (Fig. 5, Suppl. Figs. 11–12) and the van't Hoff analysis (Fig. 4) implied that fluorescence labeling leads to an altered disorderedness or flexibility of antibodies. Therefore, we determined the root mean square fluctuation (RMSF) of C_α carbon atoms for the unlabeled and fluorescently labeled antibodies revealing that labeling with AlexaFluor647, but not with AlexaFluor546, resulted in increased structural flexibility (higher RMSF values) of extended portions of trastuzumab (Fig. 7B). There was no obvious correlation between the location of the labels and the segments with increased RMSF since the right Fab arm in Fig. 7C having no increased RMSF values has four fluorescent labels, while the left Fab arm with just two fluorescent labels contains extended regions with increased RMSF values. Higher RMSF does not correlate with the labeling density of individual light or heavy chains either. Although heavy chain A has twice as many fluorophores as heavy chain C, approximately the same fraction of them exhibits heightened RMSF values. The lack of effect of AlexaFluor546 on the RMSF of the antibody is also obscure although we did find certain differences between the dynamical properties of the antibody-

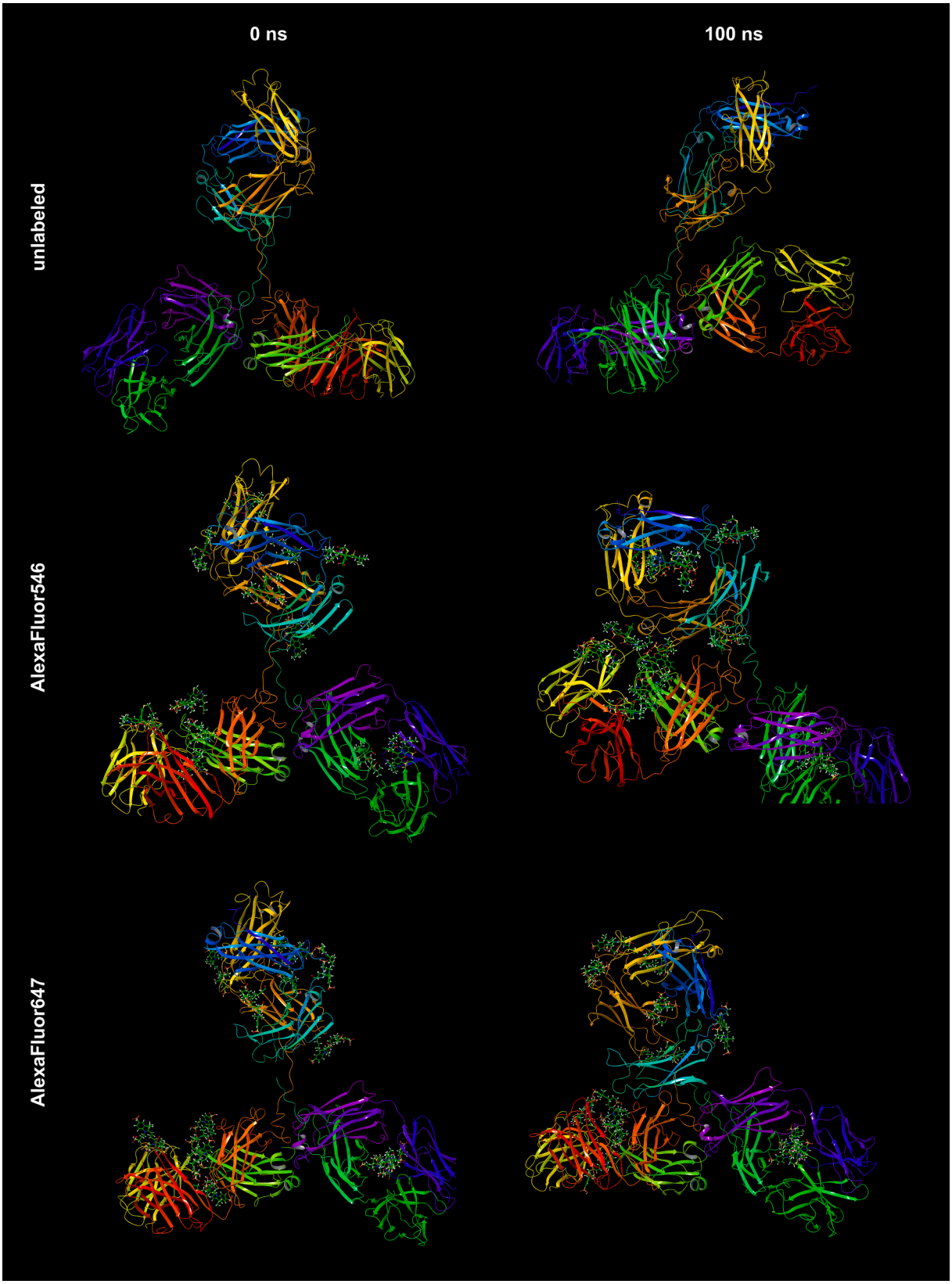

Fig. 6. Molecular dynamics simulations of unlabeled and fluorescently-labeled trastuzumab. Trastuzumab was labeled with AlexaFluor546 or AlexaFluor647 in silico, and MD simulations were carried out with both the unlabeled and the fluorescently labeled antibodies. The polypeptide backbone is shown using the ribbon representation, whereas the fluorescent dyes are displayed using ball-and-stick representation. Snapshots of the MD simulations are shown at 0 and 100 ns.

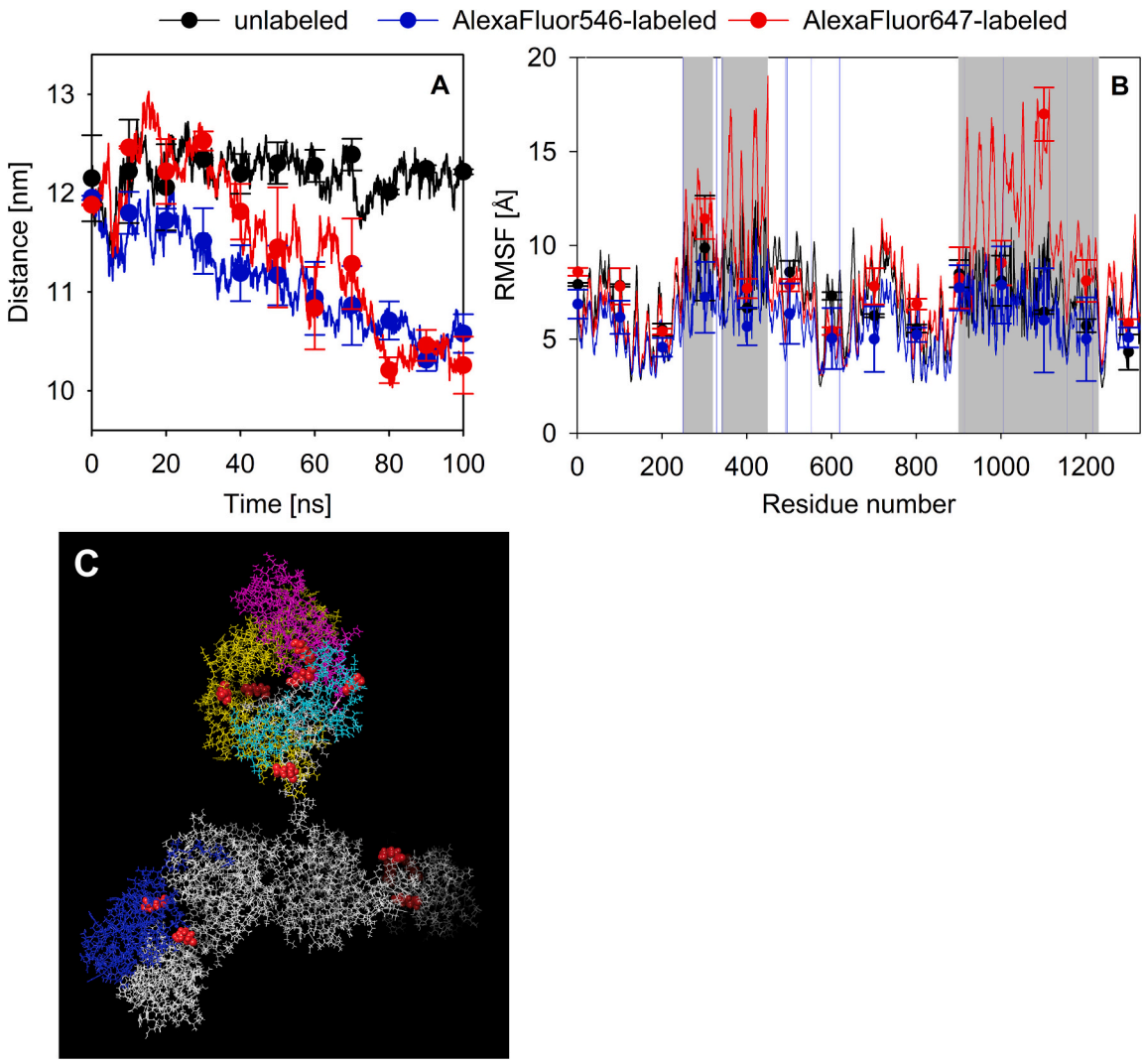

Fig. 7. Quantitative evaluation of molecular dynamics simulations. (A) The mean distance between Thr58 in the heavy chain (located in the Fc part) and Asn437 in the heavy chain (located in the epitope binding region) were calculated from the MD trajectories. The positions of these amino acids are displayed in the structure of trastuzumab in Suppl. Fig. 14. (B) The root mean square fluctuation (RMSF) of unlabeled, AlexaFluor546-, or AlexaFluor647-labeled trastuzumab was determined and it is displayed as a function of residue number. The error bars are shown for every 100th residue and correspond to the standard error of the mean calculated from the four MD simulations. The regions highlighted in gray in panel B correspond to those segments of AlexaFluor647-labeled trastuzumab in which the RMSF is larger than in the unlabeled IgG. These regions are shown in color in panel C (cyan: residues 250–320, chain A; purple: residues 340–450, chain A; yellow: residues 900–1114, chain C; blue: residues 1115–1230, chain D).

conjugated dyes. The mean RMSF of the heavy atoms in AlexaFluor546 was lower by ~25 % than that of AlexaFluor647 (Suppl. Fig. 16), although both values indicate significant degree of fluctuation (7.8 ± 0.4 Å and 9.7 ± 0.5 Å for AlexaFluor546 and AlexaFluor647, respectively). We also compared the distance of the center of mass of the two dyes to the ε-amino nitrogen of those lysines to which the dyes are conjugated. By the end of the simulations, the distance between the dyes' center of mass and the labeled lysines reached a stable value, which was larger by ~1 nm for AlexaFluor546 (Suppl. Fig. 16). In the free dyes, the distance between their center of mass and the hydroxyl oxygen in the carboxyl group (corresponding to the same distance calculated for the antibody attached fluorophores) displayed wild fluctuations without significant difference between the two dyes. Although these subtle differences between the dynamics of the two antibody-conjugated dyes might hint that they can influence local, high-frequency vibrations of the antibody, further investigations are required to reach solid conclusions. While MD simulations provided unequivocal evidence for increased structural flexibility of AlexaFluor647-conjugated trastuzumab, the lack of a similar effect for AlexaFluor546-labeled trastuzumab and the correlation between increased RMSF and dye location remain unclear.

4. Discussion

In the present manuscript, we carried out extensive functional and biophysical analysis of two antibodies (W6/32, trastuzumab) labeled by one of two fluorescent dyes (AlexaFluor546, AlexaFluor647). According to the functional investigations, all tested functions of the two antibodies decayed with remarkably similar dependence on the degree of labeling manifested in a less than linear increase in fluorescence intensity of the antibodies bound to their target as a function of the degree of labeling. This deviation is due to the combined effect of decreased fluorescence quantum efficiency and decreased antibody affinity, as modeled in a quantitative way previously [7]. The fact that decreased affinity to the target (epitope, Fcγ receptor, protein A, protein G) must play a role and that these functions decay identically with the degree of labeling suggested to us that this observation is an indication of global, fluorescence labeling-induced alterations in antibody structure. An alternative

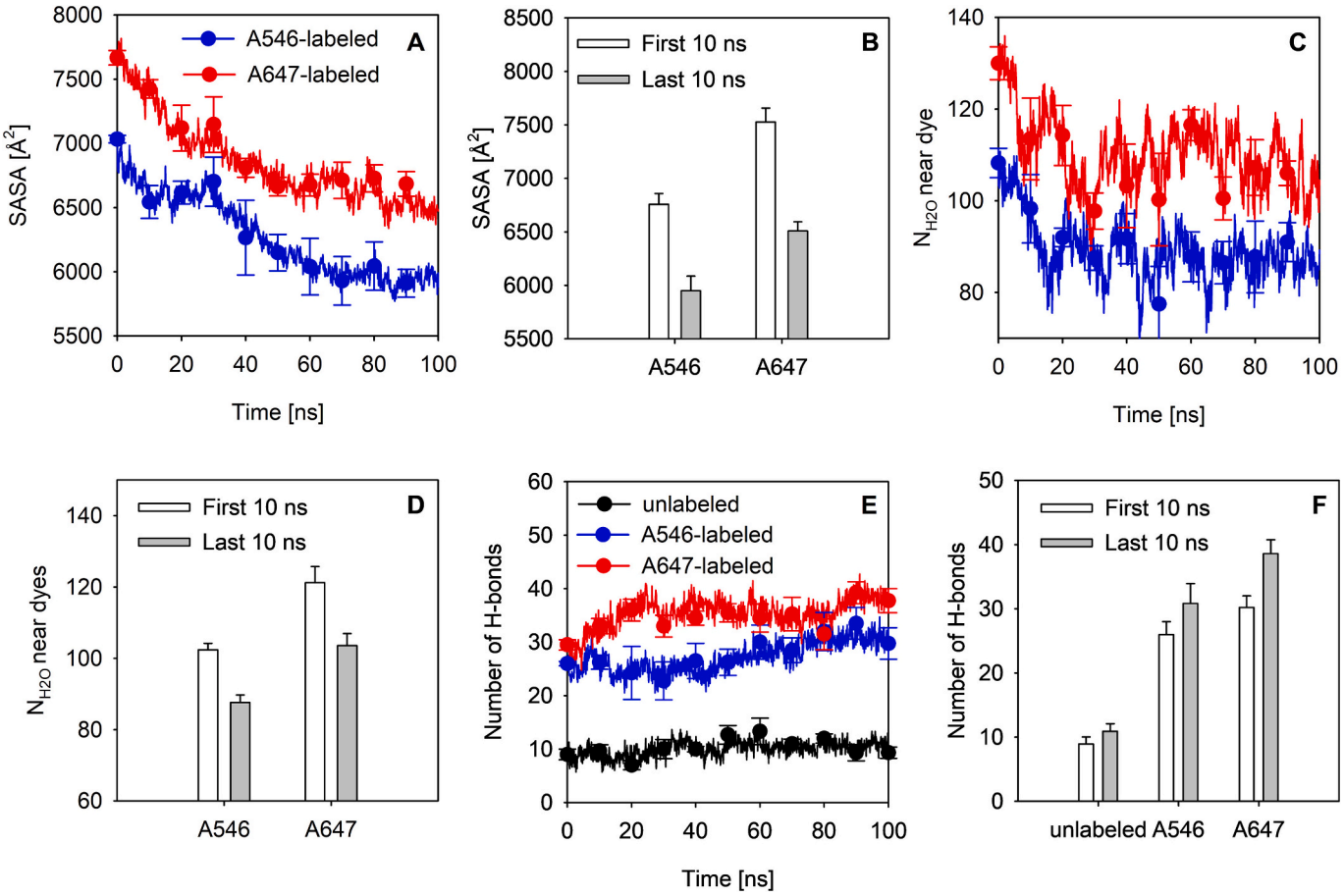

Fig. 8. Evaluation of the solvent exposure of dyes and the number of H-bonds in the antibody. The solvent accessible surface area (SASA) of the antibody-conjugated fluorescent dyes was determined, and it is plotted for both AlexaFluor546- and AlexaFluor647-labeled antibodies as a function of time (A), or as the mean during the first and last 10 ns of the simulation (B). The number of water molecules (N_{H2O}) in the 3 Å-vicinity of the dyes is displayed as a function of simulation time (C), or as the mean during the first and last 10 ns of the simulation (D). The number of hydrogen bonds was determined in the whole antibody structure, and it is plotted as a function of time (E), or as the mean during the first and last 10 ns of the simulation (F). The error bars display the standard error of the mean in each bar graph, and they also correspond to the standard error of the mean of every 100th data point in the line graphs. The standard error of the mean was calculated from the four MD simulations.

explanation could be steric hindrance: key lysine residues near all the tested functional sites —including the hypervariable region and the binding sites for protein A, protein G, and Fcγ receptor—may be labeled with equal probability, thus similarly affecting these functions. Although we did not identify the labeled lysines and cannot fully exclude this possibility, it appears highly unlikely given the known variability in lysine labeling efficiencies [49,50]. Moreover, both experimental and simulation data consistently indicate that fluorescence labeling induces global structural changes in the antibody, supporting this as the more plausible explanation. The major alterations identified were as follows: (i) fluorescence labeling results in a more compact antibody structure according to the FRET experiments and the MD simulations; (ii) anisotropy decay data suggested that conjugation of fluorescent dyes leads to accelerated flexible motions of the antibody in the 10–40-ns time range; (iii) the melting temperature of the Fab and Fc domains is not altered by fluorescence labeling; (iv) binding of trastuzumab to a soluble antigenic peptide is enthalpically favored but entropically unfavorable, and fluorescence labeling makes the binding less favored enthalpically and less punished entropically. The Gibbs free energy of binding and consequently antibody affinity are a function of enthalpic and entropic contributions. The latter contains contributions from the antibody, the antigen and the hydrating water molecules [51]. Although the role of the changed hydration pattern is extremely difficult to predict [52], an obvious explanation for the entropy penalty in binding, i.e., the less disordered nature of the bound state, is easy to account for by assuming that the bound antigen has limited motional freedom. Given the complicated nature of these changes, only a plausible explanation for the lower entropy penalty and lower magnitude of enthalpy decrease in fluorescent antibodies can be offered. According to this proposition, fluorescence labeling-induced structural alterations in antibody structure, supported by the MD simulations, result in less favored antibody-antigen binding manifested in a lower magnitude of enthalpy decrease during antigen binding (lower bond or interaction energy). If antigen binding is less optimal, the motion of the hypervariable region and the antigen will be less restricted leading to a smaller entropy penalty.

The FRET experiments revealed that the distance between the Fc and the hypervariable regions is smaller in fluorescently labeled antibodies than in their unlabeled counterparts. The fact that this experimental observation is supported by the MD simulations and that the calculated distances are in accordance with the size of an IgG present convincing evidence for the reliability of these conclusions. The distance between the Fc and the hypervariable regions was measured by fluorescently labeling the Fc part and the antigen. Interpretation of FRET experiments in which formation of the antibody-antigen complex is not complete, i.e., free antigen is present, must consider the contribution of free dyes (dyes conjugated to antigen not bound to the antibody). To avoid a large population of free donors (and the resulting drop in FRET efficiency), the antigen was labeled with the acceptor rather than the donor. The presence of free acceptors did not have any significant contribution to the

measured FRET efficiency since the probability of a free acceptor-labeled antigen being randomly within nanometer distance from an antibody is negligible (see the section "Determination of the extent of FRET due to high concentration of free acceptors" in the Supplementary materials). This conclusion is further corroborated by the observation that an excess of unlabeled H98 displaced acceptor-conjugated H98 from trastuzumab, thereby abolishing FRET between the antigen and the antibody's Fc region. Therefore, the measured FRET efficiency can be attributed to FRET taking place in the complex of the antigen and the antibody.

The time-dependent anisotropy decay experiments revealed that flexible motions of fluorescent antibodies in the 10–40-ns range are faster than those in unlabeled antibodies. In order to unequivocally attribute the accelerated anisotropy decay to faster intramolecular motions, we had to exclude other possible mechanisms leading to an increased rate of anisotropy decay: (i) the rotational correlation time of an antibody is ~150 ns [42], therefore rotation of the whole molecule is too slow to lead to anisotropy decay in the time range up to 50 ns; (ii) We also considered two possible sources of artifacts affecting the fast anisotropy decay components with time constants in the subnanosecond-couple of nanoseconds range. One of them was the presence of free, non-antibody-conjugated dye in the fluorescent antibody samples, whose rotational correlation time, and consequently the anisotropy decay time constant, is $V\eta/(kT) \approx 0.3$ ns assuming the volume of the free dye $(V) = 4/3\pi \cdot (0.7\ \text{nm})^3$, and the viscosity of water at 25 °C $(\eta) = 8.93{\cdot}10^{-4}$ Pa s, in accordance with experimentally determined values for dyes of similar size [53]. Although considerable effort was made to remove unbound dye molecules, the presence of trace amounts of free dye in the samples cannot be entirely excluded. However, the extreme fast anisotropy decay of free dye is unlikely to interfere with the accurate determination of the anisotropy decay constants in the time range above 10 ns. Furthermore, inclusion of an additional size-exclusion chromatography step in the purification of the labeled antibodies, beyond those applied in the standard protocol, did not result in any substantial change in the anisotropy decay components (data not shown). As a second mechanism affecting anisotropy decay in the nanosecond time range we considered that high fluorophore density on the surface of antibodies with a high degree of labeling leads to increased homo-FRET resulting in accelerated anisotropy decay [54]. However, anisotropy decay due to homo-FRET is twice faster than the homo-FRET rate and therefore it is expected to be manifested in faster anisotropy decay in the nanosecond time range [43]. Furthermore, we also compared the anisotropy decays in two different kinds of highly labeled antibodies. One of them was labeled to a high degree only with AlexaFluor546, while the other was labeled to a similar degree with a mixture of AlexaFluor546 and AlexaFluor488. Due to the lower number of AlexaFluor546 on the latter, the probability of homo-FRET is lower than in the former. Although there was a small difference between the time constants of the slow anisotropy decay components of these two differently labeled antibodies, the anisotropy decay in the 10–40-ns time range of the antibody labeled with a mixture of two different kinds of dyes to a high degree of labeling was still faster than in lowly labeled antibodies. These observations and arguments imply that fluorescence labeling indeed accelerates molecular motions of antibodies in the 10–40-ns time range. Several different molecular motions have been observed in IgGs in this time range including the motion and rotation of the Fab and Fc parts relative to each other and intradomain motions termed elbow bending [42,44,45]. The fact that the slow anisotropy decay component was also present in fluorescent Fab fragments suggests that intradomain elbow bending or other kinds of intradomain flexibility must be behind the observation. Several studies suggested that high antigen affinity in antibodies is achieved by restricted flexibility [18–21]. Assuming that the affinity of the studied antibodies is indeed correlated with their higher rigidity, the increased flexibility of fluorescently labeled antibodies may provide a mechanistic explanation for their reduced affinity.

MD simulations provided convincing evidence for the fluorescence labeling-induced global alterations in antibody structure. The Fab and Fc regions of unlabeled trastuzumab exhibited dynamic movement without permanently adhering to one another. However, when AlexaFluor546 or AlexaFluor647 was conjugated to the in-silico structure of trastuzumab, the Fab and Fc regions collapsed persistently onto each other without gross alterations in the structure of the Fab and Fc domains. This latter observation is in accordance with the lack of any effect of fluorescence labeling on the melting temperature of these domains according to nanoDSF measurements. During the simulations, the solvent accessible surface area of the dyes and the number of water molecules around the dyes decreased, suggesting that the hydrophobic effect was the underlying cause. The hydrophobic effect between dyes attached to the Fab and Fc fragments can directly cause these domains to adhere, as demonstrated in Supplementary Movie 2 showing AlexaFluor546-labeled trastuzumab. Alternatively, the dyes may influence the internal dynamics of the Fab and Fc domains through the hydrophobic effect, as suggested by Supplementary Movie 3, featuring AlexaFluor647-labeled trastuzumab. Evidence for alterations in the internal dynamics of IgG domains includes the increased RMSF observed in AlexaFluor647-labeled trastuzumab and the higher number of hydrogen bonds detected for both AlexaFluor546- and AlexaFluor647-conjugated antibodies. A large body of evidence suggests that contacts between distant parts of IgGs affects antigen binding to the hypervariable region [13–16]. The hydrophobic effect-dependent collapse of antibody structure together with increased dynamism may provide the structural background for the decreased affinity of fluorescently labeled antibodies by interfering with the aforementioned interactions required for antigen binding. It is of interest to note that clustering of antibody-conjugated dyes, probably mediated by the hydrophobic effect, results in their reduced fluorescence [7,55], and the same hydrophobic effect seems to be the reason for the reduced affinity of fluorescently-labeled antibodies. Independent of whether hydrophobic-effect mediated structural collapse or increased molecular motions and flexibility are behind the labeling-dependent decreased antibody affinity, the observation of glycerol partially decreasing the effect of fluorescence labeling on antibody affinity can be explained since glycerol is known to reduce the hydrophobic effect [37] and dampen large scale fluctuations due to increased viscosity [56–58].

In conclusion, the results presented in the manuscript reveal that fluorescence labeling induces global alterations in the structure of antibodies due to the hydrophobic effect and increased structural dynamics (Fig. 9). These findings are useful for scientists who aim to apply labeled antibodies in research or therapy, develop optimized labeling strategies, or explore the structure-function relationships of labeled

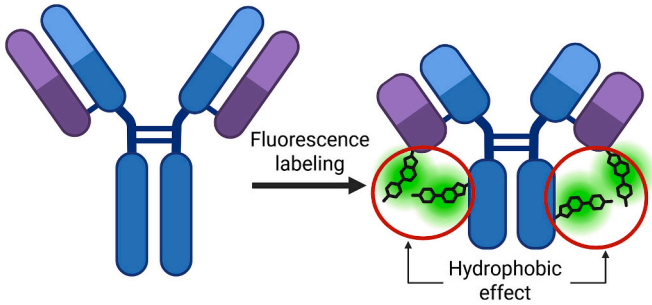

Fig. 9. Schematic representation of the structural changes induced by fluorescence antibody labeling. Conjugation of fluorescent dyes to antibodies brings about global alterations in the structure of antibodies resulting in altered dynamics and movement of the Fab and Fc parts closer to each other seen as a collapse of antibody structure. These structural changes are induced by the hydrophobic interactions between dye molecules. The figure is not drawn to scale and alterations are exaggerated for viewing purposes.
(Created in BioRender. Nagy, P. (2025) https://BioRender.com/l09fuf2).

antibodies.

Supplementary data to this article can be found online at https://doi.org/10.1016/j.ijbiomac.2025.146209.

CRediT authorship contribution statement

Tímea Hajdu: Writing – original draft, Investigation, Formal analysis. **István Rebenku:** Investigation, Formal analysis. **Tayde Gabriela Serrano Cano:** Visualization, Investigation, Formal analysis. **Gábor Mocsár:** Investigation, Formal analysis. **Bálint Bécsi:** Writing – original draft, Investigation, Formal analysis. **Ferenc Erdődi:** Supervision. **Peter Nagy:** Writing – review & editing, Supervision, Funding acquisition, Conceptualization.

Funding

The work reported in the manuscript has been supported by the National Research, Development and Innovation Office, Hungary (ANN133421, K138075 to PN) and by the University of Debrecen.

Declaration of competing interest

The authors declare the following financial interests/personal relationships which may be considered as potential competing interests: Peter Nagy reports financial support was provided by National Research, Development and Innovation Office, Hungary. If there are other authors, they declare that they have no known competing financial interests or personal relationships that could have appeared to influence the work reported in this paper.

Data availability

Data will be made available on request.

References

[1] R.P. Haugland, Coupling of monoclonal antibodies with fluorophores, Methods Mol. Biol. 45 (1995) 205–221.
[2] G.T. Hermanson, Chapter 1 - Introduction to Bioconjugation, in: Bioconjugate Techniques, Third edition, Academic Press, Boston, 2013, pp. 1–125.
[3] J.E. Berlier, A. Rothe, G. Buller, J. Bradford, D.R. Gray, B.J. Filanoski, W.G. Telford, S. Yue, J. Liu, C.Y. Cheung, W. Chang, J.D. Hirsch, J.M. Beechem, R.P. Haugland, Quantitative comparison of long-wavelength Alexa Fluor dyes to cy dyes: fluorescence of the dyes and their bioconjugates, J. Histochem. Cytochem. 51 (12) (2003) 1699–1712.
[4] R.I. MacDonald, Characteristics of self-quenching of the fluorescence of lipid-conjugated rhodamine in membranes, J. Biol. Chem. 265 (23) (1990) 13533–13539.
[5] H.J. Gruber, C.D. Hahn, G. Kada, C.K. Riener, G.S. Harms, W. Ahrer, T.G. Dax, H. G. Knaus, Anomalous fluorescence enhancement of Cy3 and cy3.5 versus anomalous fluorescence loss of Cy5 and Cy7 upon covalent linking to IgG and noncovalent binding to avidin, Bioconjug. Chem. 11 (5) (2000) 696–704.
[6] R. Luchowski, E.G. Matveeva, I. Gryczynski, E.A. Terpetschnig, L. Patsenker, G. Laczko, J. Borejdo, Z. Gryczynski, Single molecule studies of multiple-fluorophore labeled antibodies, Effect of homo-FRET on the number of photons available before photobleaching, Curr Pharm Biotechnol 9 (5) (2008) 411–420.
[7] A. Szabó, T. Szendi-Szatmári, L. Ujlaky-Nagy, I. Rádi, G. Vereb, J. Szöllősi, P. Nagy, The effect of fluorophore conjugation on antibody affinity and the photophysical properties of dyes, Biophys. J. 114 (3) (2018) 688–700.
[8] T. McCormack, G. O'Keeffe, B. Mac Craith, R. O'Kennedy, Assessment of the effect of increased fluorophore labelling on the binding ability of an antibody, Anal. Lett. 29 (6) (1996) 953–968.
[9] S. Vira, E. Mekhedov, G. Humphrey, P.S. Blank, Fluorescent-labeled antibodies: balancing functionality and degree of labeling, Anal. Biochem. 402 (2) (2010) 146–150.
[10] D. Shrestha, A. Bagosi, J. Szöllősi, A. Jenei, Comparative study of the three different fluorophore antibody conjugation strategies, Anal. Bioanal. Chem. 404 (5) (2012) 1449–1463.
[11] W.K. Wong, J. Leem, C.M. Deane, Comparative analysis of the CDR loops of antigen receptors, Front. Immunol. 10 (2019) 2454.
[12] G. Vidarsson, G. Dekkers, T. Rispens, IgG subclasses and allotypes: from structure to effector functions, Front. Immunol. 5 (2014) 520.
[13] I. Sela-Culang, V. Kunik, Y. Ofran, The structural basis of antibody-antigen recognition, Front. Immunol. 4 (2013) 302.
[14] A. Janda, A. Bowen, N.S. Greenspan, A. Casadevall, Ig constant region effects on variable region structure and function, Front. Microbiol. 7 (2016) 22.
[15] O. Pritsch, C. Magnac, G. Dumas, J.P. Bouvet, P. Alzari, G. Dighiero, Can isotype switch modulate antigen-binding affinity and influence clonal selection? Eur. J. Immunol. 30 (12) (2000) 3387–3395.
[16] R. Huber, J. Deisenhofer, P.M. Colman, M. Matsushima, W. Palm, Crystallographic structure studies of an IgG molecule and an fc fragment, Nature 264 (5585) (1976) 415–420.
[17] Y. Xia, A. Janda, E. Eryilmaz, A. Casadevall, C. Putterman, The constant region affects antigen binding of antibodies to DNA by altering secondary structure, Mol. Immunol. 56 (1–2) (2013) 28–37.
[18] V. Manivel, N.C. Sahoo, D.M. Salunke, K.V. Rao, Maturation of an antibody response is governed by modulations in flexibility of the antigen-combining site, Immunity 13 (5) (2000) 611–620.
[19] T. Li, M.B. Tracka, S. Uddin, J. Casas-Finet, D.J. Jacobs, D.R. Livesay, Rigidity emerges during antibody evolution in three distinct antibody systems: evidence from QSFR analysis of fab fragments, PLoS Comput. Biol. 11 (7) (2015) e1004327.
[20] M.L. Fernandez-Quintero, J.R. Loeffler, L.M. Bacher, F. Waibl, C.A. Seidler, K. R. Liedl, Local and global rigidification upon antibody affinity maturation, Front. Mol. Biosci. 7 (2020) 182.
[21] J. Zimmermann, F.E. Romesberg, C.L. Brooks 3rd, I.F. Thorpe, Molecular description of flexibility in an antibody combining site, J. Phys. Chem. B 114 (21) (2010) 7359–7370.
[22] B. Jiang, W. Liu, H. Qu, L. Meng, S. Song, T. Ouyang, C. Shou, A novel peptide isolated from a phage display peptide library with trastuzumab can mimic antigen epitope of HER-2, J. Biol. Chem. 280 (6) (2005) 4656–4662.
[23] J.Z. Hui, S. Tamsen, Y. Song, A. Tsourkas, LASIC: light activated site-specific conjugation of native IgGs, Bioconjug. Chem. 26 (8) (2015) 1456–1460.
[24] R. Nezlin, V. Ghetie, Interactions of immunoglobulins outside the antigen-combining site, Adv. Immunol. 82 (2004) 155–215.
[25] J. Deisenhofer, Crystallographic refinement and atomic models of a human fc fragment and its complex with fragment B of protein a from Staphylococcus aureus at 2.9- and 2.8-a resolution, Biochemistry 20 (9) (1981) 2361–2370.
[26] A.E. Sauer-Eriksson, G.J. Kleywegt, M. Uhlen, T.A. Jones, Crystal structure of the C2 fragment of streptococcal protein G in complex with the fc domain of human IgG, Structure 3 (3) (1995) 265–278.
[27] B.D. Wines, M.S. Powell, P.W. Parren, N. Barnes, P.M. Hogarth, The IgG fc contains distinct fc receptor (FcR) binding sites: the leukocyte receptors fc gamma RI and fc gamma RIIa bind to a region in the fc distinct from that recognized by neonatal FcR and protein a, J. Immunol. 164 (10) (2000) 5313–5318.
[28] J.R. Lakowicz, Fluorescence Anisotropy, in: Principles of Fluorescence Spectroscopy, Springer, New York, 2006, pp. 353–382.
[29] Z. Gryczynski, I. Gryczynski, Fluorescence: Time-Resolved Phenomena, in: Practical Fluorescence Spectroscopy, CRC Press, Boca Raton, 2020, pp. 525–631.
[30] S. Hetey, B. Boros-Olah, T. Kuik-Rozsa, Q. Li, Z. Karanyi, Z. Szabo, J. Roszik, N. Szaloki, G. Vamosi, K. Toth, L. Szekvolgyi, Biophysical characterization of histone H3.3 K27M point mutation, Biochem. Biophys. Res. Commun. 490 (3) (2017) 868–875.
[31] T. Szendi-Szatmári, A. Szabó, J. Szöllősi, P. Nagy, Reducing the detrimental effects of saturation phenomena in FRET microscopy, Anal. Chem. 91 (9) (2019) 6378–6382.
[32] A. Fábián, G. Horváth, G. Vámosi, G. Vereb, J. Szöllősi, TripleFRET measurements in flow cytometry, Cytometry A 83 (4) (2013) 375–385.
[33] J. Liu, Y. Lu, FRET study of a trifluorophore-labeled DNAzyme, J. Am. Chem. Soc. 124 (51) (2002) 15208–15216.
[34] J.P. Brandt, T.W. Patapoff, S.R. Aragon, Construction, MD simulation, and hydrodynamic validation of an all-atom model of a monoclonal IgG antibody, Biophys. J. 99 (3) (2010) 905–913.
[35] W. Humphrey, A. Dalke, K. Schulten, VMD: visual molecular dynamics, J. Mol. Graph. 14 (1) (1996) (33–8, 27-8).
[36] D. Frishman, P. Argos, Knowledge-based protein secondary structure assignment, Proteins 23 (4) (1995) 566–579.
[37] V. Vagenende, M.G. Yap, B.L. Trout, Mechanisms of protein stabilization and prevention of protein aggregation by glycerol, Biochemistry 48 (46) (2009) 11084–11096.
[38] K. Gekko, S.N. Timasheff, Thermodynamic and kinetic examination of protein stabilization by glycerol, Biochemistry 20 (16) (1981) 4677–4686.
[39] V. Vagenende, A.X. Han, H.B. Pek, B.L. Loo, Quantifying the molecular origins of opposite solvent effects on protein-protein interactions, PLoS Comput. Biol. 9 (5) (2013) e1003072.
[40] Y. Hamuro, M.G. Derebe, S. Venkataramani, J.F. Nemeth, The effects of intramolecular and intermolecular electrostatic repulsions on the stability and aggregation of NISTmAb revealed by HDX-MS, DSC, and nanoDSF, Protein Sci. 30 (8) (2021) 1686–1700.
[41] S. Lisina, W. Inam, M. Huhtala, F. Howaili, H. Zhang, J.M. Rosenholm, Nano differential scanning Fluorimetry as a rapid stability assessment tool in the Nanoformulation of proteins, Pharmaceutics 15 (5) (2023).
[42] D.C. Hanson, J. Yguerabide, V.N. Schumaker, Segmental flexibility of immunoglobulin G antibody molecules in solution: a new interpretation, Biochemistry 20 (24) (1981) 6842–6852.
[43] S.S. Vogel, C. Thaler, P.S. Blank, V. Koushik, Time-resolved fluorescence anisotropy, in: A. Periasamy, R.M. Clegg (Eds.), FLIM Microscopy in Biology and Medicine, CRC Press, Boca Raton, 2010, pp. 245–288.
[44] J. Yguerabide, H.F. Epstein, L. Stryer, Segmental flexibility in an antibody molecule, J. Mol. Biol. 51 (3) (1970) 573–590.

[45] Y. Hayashi, S. Yagihara, Elbow- and hinge-bending motions of IgG: dielectric response and dynamic feature, Biopolymers 105 (9) (2016) 626–632.
[46] C.A. Sotriffer, B.M. Rode, J.M. Varga, K.R. Liedl, Elbow flexibility and ligand-induced domain rearrangements in antibody fab NC6.8: large effects of a small hapten, Biophys. J. 79 (2) (2000) 614–628.
[47] O. Olaleye, C. Graf, B. Spanov, N. Govorukhina, M.R. Groves, N.C. van de Merbel, R. Bischoff, Determination of binding sites on trastuzumab and pertuzumab to selective affimers using hydrogen-deuterium exchange mass spectrometry, J. Am. Soc. Mass Spectrom. 34 (4) (2023) 775–783.
[48] P. Bork, L. Holm, C. Sander, The immunoglobulin fold, Structural classification, sequence patterns and common core, J Mol Biol 242 (4) (1994) 309–320.
[49] V. Gautier, A.J. Boumeester, P. Lossl, A.J. Heck, Lysine conjugation properties in human IgGs studied by integrating high-resolution native mass spectrometry and bottom-up proteomics, Proteomics 15 (16) (2015) 2756–2765.
[50] J.J. Hill, T.L. Tremblay, C.R. Corbeil, E.O. Purisima, T. Sulea, An accurate TMT-based approach to quantify and model lysine susceptibility to conjugation via N-hydroxysuccinimide esters in a monoclonal antibody, Sci. Rep. 8 (1) (2018) 17680.
[51] J.D. Chodera, D.L. Mobley, Entropy-enthalpy compensation: role and ramifications in biomolecular ligand recognition and design, Annu. Rev. Biophys. 42 (2013) 121–142.
[52] B. Wienen-Schmidt, H.R.A. Jonker, T. Wulsdorf, H.D. Gerber, K. Saxena, D. Kudlinzki, S. Sreeramulu, G. Parigi, C. Luchinat, A. Heine, H. Schwalbe, G. Klebe, Paradoxically, Most flexible ligand binds Most entropy-favored: intriguing impact of ligand flexibility and solvation on drug-kinase binding, J. Med. Chem. 61 (14) (2018) 5922–5933.
[53] S. Ghosh, A. Roy, D. Banik, N. Kundu, J. Kuchlyan, A. Dhir, N. Sarkar, How does the surface charge of ionic surfactant and cholesterol forming vesicles control rotational and translational motion of rhodamine 6G perchlorate (R6G ClO(4))? Langmuir 31 (8) (2015) 2310–2320.
[54] D.S. Lidke, P. Nagy, B.G. Barisas, R. Heintzmann, J.N. Post, K.A. Lidke, A. H. Clayton, D.J. Arndt-Jovin, T.M. Jovin, Imaging molecular interactions in cells by dynamic and static fluorescence anisotropy (rFLIM and emFRET), Biochem. Soc. Trans. 31 (Pt 5) (2003) 1020–1027.
[55] M. Ogawa, N. Kosaka, P.L. Choyke, H. Kobayashi, H-type dimer formation of fluorophores: a mechanism for activatable, in vivo optical molecular imaging, ACS Chem. Biol. 4 (7) (2009) 535–546.
[56] M. Pozar, B. Lovrincevic, Structure and dynamics in aqueous mixtures of glycerol: insights from molecular dynamics simulations, Soft Matter 20 (40) (2024) 8061–8067.
[57] D. Demuth, N. Haase, D. Malzacher, M. Vogel, Effects of solvent concentration and composition on protein dynamics: 13C MAS NMR studies of elastin in glycerol-water mixtures, Biochim. Biophys. Acta 1854 (8) (2015) 995–1000.
[58] M. Tarek, D.J. Tobias, The role of protein-solvent hydrogen bond dynamics in the structural relaxation of a protein in glycerol versus water, Eur. Biophys. J. 37 (5) (2008) 701–709.

SUPPLEMENTARY INFORMATION

Fluorescence labeling-induced structural rearrangement of a monoclonal IgG revealed by biophysical experiments and simulations

[1]Tímea Hajdu, [1]István Rebenku, [1]Tayde Gabriela Serrano Cano, [1]Gábor Mocsár, [2]Bálint Bécsi, [2]Ferenc Erdődi, [1*]Peter Nagy

[1]Department of Biophysics and Cell Biology, Faculty of Medicine, University of Debrecen, Debrecen, Hungary

[2]Department of Medical Chemistry, Faculty of Medicine, University of Debrecen, Debrecen, Hungary

Supplementary Methods

Preparation of Fab fragments

Briefly, the spin column containing immobilized papain was equilibrated with Digestion Buffer, and the IgG to be digested was passed through a "Zeba" Spin Desalting Column equilibrated with Digestion Buffer, followed by applying this ion exchanged IgG sample onto the spin column containing the immobilized papain. Digestion was allowed to reach completion in 2-5 hours depending on the amount of IgG to be digested at 37°C on a tabletop rocker. At the end of the incubation, the spin column was centrifuged to allow collection of the digested products in the flow-through. Finally, this mixture was applied to an NAb Protein A Plus Spin Column binding undigested IgG and the Fc fragments. The purified Fab preparation was collected in the flow-through.

Labeling of antibodies with fluorescent dyes

The labeling mixture was prepared by adding 75 μL of 1 M carbonate buffer, the antibody to be labeled to a final concentration of 2 mg/mL and PBS so that the final volume was 750 μL. Depending on the degree of labeling to be achieved, 3-10 μL of the N-Hydroxysuccinimide derivative of the dye was added to the mixture followed by a 1-hour incubation at 25°C under constant agitation. Unreacted dye molecules were removed by passing the reaction mixture through a Sephadex G-50 column (Sigma-Aldrich, GE17-0043-02) removing molecules smaller than ~30 kDa from the mixture [1] followed by cleaning up the flow-through of the previous purification step using a BioRad BioSpin 30 column (BioRad, #7326231). Given that the fractionation range of this prepackaged column is 2.5-40 kDa and that the molecular weight of free AlexaFluor dyes is smaller than 2.5 kDa (molecular weight of AlexaFluor546 and AlexaFluor647 are 1159 g/mol and 1250 g/mol, respectively, according to ThermoFisher [2]), it fully (~98%) retains unreacted dye molecules smaller than the lower boundary of the fractionation range.

Determination of the degree of labeling of single- and double-labeled antibodies by spectrophotometry

For antibodies labeled by a single kind of dye, the absorbance of the labeled antibody stock was measured at two wavelengths corresponding to the absorption maximum of the dye and to the absorption of amino acids absorbing in the UV range (280 nm):

$$A\left(\lambda_{dye}\right) = A_{dye}\left(\lambda_{dye}\right) = \varepsilon_{dye}\ c_{dye,\mathrm{M}}\ L \tag{S1}$$

$$A(280) = A_{IgG}(280) + A_{dye}(280) = \varepsilon_{IgG}\ c_{IgG,\mathrm{M}}\ \mathrm{L} + A_{dye}\left(\lambda_{dye}\right)\ CF \tag{S2}$$

where A is the optical density of the species specified in the subscript measured at a wavelength specified in parentheses. $\varepsilon_{\mathrm{IgG}}$ is the molar absorption coefficient of the antibody at 280 nm and $\varepsilon_{\mathrm{dye}}$ is the molar absorption coefficient of the dye at its absorption maximum. $c_{\mathrm{dye,M}}$ and $c_{\mathrm{IgG,M}}$ are the molar concentrations of the dye and the antibody, respectively, L is the optical path length in cm and CF is a correction factor specifying the relative optical density of the dye at 280 nm compared to its absorption at its absorption maximum. These correction factors are available from the manufacturer or can be determined by measuring the absorption spectrum of the free dye. If the optical density of the dye at its absorption maximum is above two OD units, the stock solution must be diluted, and the calculation must take this dilution factor (DF) into consideration. Equation (S2) can be rearranged to provide the molar concentration of the antibody:

$$c_{IgG,\mathrm{M}} = \frac{A(280) - A_{dye}\left(\lambda_{dye}\right)\ CF}{\varepsilon_{IgG}\ \mathrm{L}} DF \tag{S3}$$

The molar extinction coefficient of an IgG is ~203,000 $M^{-1}cm^{-1}$. If a significant amount of Rayleigh or Tyndall scattering, due to the presence of antibody aggregates, is present, judged by the gradually increasing optical density of the sample towards low wavelengths in between the absorption peaks of the dye and the antibody, the measured absorbance values will be higher than the real absorbance of the stock. This phenomenon especially affects the values in or close to the UV range (e.g., the 280-nm peak of the antibody). Ultracentrifugation of the sample to get rid of aggregates or correction for light scattering in the spectrum (e.g., https://www.fluortools.com/software/ae-uv-vis-ir-spectral-software) must be performed to make the absorbance values reliable.

Similarly, the molar concentration of the dye in the labeled stock solution can be determined from equation (S1):

$$c_{dye,\mathrm{M}} = \frac{A\left(\lambda_{dye}\right)\ DF}{\varepsilon_{dye}\ L} \tag{S4}$$

The average degree of labeling of the stock is the ratio of the two molar concentrations:

$$DOL = \frac{c_{dye,\mathrm{M}}}{c_{IgG,\mathrm{M}}} \tag{S5}$$

To express antibody concentration in the typically used unit of mg/mL, the molar concentration ($c_{\mathrm{IgG,M}}$) must be multiplied by the molecular weight of the IgG:

$$c_{IgG,\mathrm{mg/ml}} = c_{IgG,\mathrm{M}}\ 1.5\cdot 10^{5}\ \ \mathrm{g/mol} \tag{S6}$$

A typical calculation of the degree of labeling is presented in Supplementary Figure 1.

For antibodies labeled by two fluorescent dyes, the following system of equations describes their optical densities at the peak absorption of the two fluorophores and at the UV absorption wavelength of the antibody:

$$\begin{aligned}
A\left(\lambda_{dye1}\right) &= \varepsilon_{dye1}\left(\lambda_{dye1}\right)\ c_{dye1,\mathrm{M}}\ L + \varepsilon_{dye2}\left(\lambda_{dye1}\right)\ c_{dye2,\mathrm{M}}\ L \\
A\left(\lambda_{dye2}\right) &= \varepsilon_{dye1}\left(\lambda_{dye2}\right)\ c_{dye1,\mathrm{M}}\ L + \varepsilon_{dye2}\left(\lambda_{dye2}\right)\ c_{dye2,\mathrm{M}}\ L \\
A\left(280\right) &= \varepsilon_{dye1}\left(280\right)\ c_{dye1,\mathrm{M}}\ L + \varepsilon_{dye2}\left(280\right)\ c_{dye2,\mathrm{M}}\ L + \varepsilon_{IgG}\left(280\right)\ c_{IgG,\mathrm{M}}\ \mathrm{L}
\end{aligned} \tag{S7}$$

The subscripts define the molecular species, and the number or the variable in parentheses specify the wavelength of the measurement. For easier presentation, the equation set can be converted to a matrix equation:

$$\begin{pmatrix} A\left(\lambda_{dye1}\right) \\ A\left(\lambda_{dye2}\right) \\ A\left(280\right) \end{pmatrix} = \begin{pmatrix} \varepsilon_{dye1}\left(\lambda_{dye1}\right) & \varepsilon_{dye2}\left(\lambda_{dye1}\right) & 0 \\ \varepsilon_{dye1}\left(\lambda_{dye2}\right) & \varepsilon_{dye2}\left(\lambda_{dye2}\right) & 0 \\ \varepsilon_{dye1}\left(280\right) & \varepsilon_{dye2}\left(280\right) & \varepsilon_{IgG}\left(280\right) \end{pmatrix} \begin{pmatrix} c_{dye1,\mathrm{M}} \\ c_{dye2,\mathrm{M}} \\ c_{IgG,\mathrm{M}} \end{pmatrix} L \tag{S8}$$

Using the following designations

$$\mathbf{A} = \begin{pmatrix} A\left(\lambda_{dye1}\right) \\ A\left(\lambda_{dye2}\right) \\ A\left(280\right) \end{pmatrix},\ \boldsymbol{\varepsilon} = \begin{pmatrix} \varepsilon_{dye1}\left(\lambda_{dye1}\right) & \varepsilon_{dye2}\left(\lambda_{dye1}\right) & 0 \\ \varepsilon_{dye1}\left(\lambda_{dye2}\right) & \varepsilon_{dye2}\left(\lambda_{dye2}\right) & 0 \\ \varepsilon_{dye1}\left(280\right) & \varepsilon_{dye2}\left(280\right) & \varepsilon_{IgG}\left(280\right) \end{pmatrix},\ \mathbf{c} = \begin{pmatrix} c_{dye1,\mathrm{M}} \\ c_{dye2,\mathrm{M}} \\ c_{IgG,\mathrm{M}} \end{pmatrix} \tag{S9}$$

the equation can be written in shorter form:

$$\mathbf{A} = \boldsymbol{\varepsilon}\ \mathbf{c}\ L \tag{S10}$$

The molar concentrations can be calculated according to the following equation:

$$\mathbf{c} = \frac{\boldsymbol{\varepsilon}^{-1}\ \mathbf{A}}{L} \tag{S11}$$

Fitting a single site-two ligand model

A single target (*T*) was assumed to bind two ligands (*L1*, *L2*) with two different dissociation constants (K_{d1}, K_{d2}) according to the following equations describing equilibrium binding:

$$\begin{aligned} L1\ T &= K_{d1}\ L1T \\ L2\ T &= K_{d2}\ L2T \\ L1_{tot} &= L1 + L1T \\ L2_{tot} &= L2 + L2T \\ T_{tot} &= L1T + L2T + T \end{aligned} \tag{S12}$$

where *L1T* and *L2T* are the concentration of complexes formed by the first and second ligand with the target, respectively, and the variables with "tot" in the subscript designate the total concentration of the respective entity. The equation set allows for depletion of any of the ligands. This feature was necessary since the same equation set was used for characterizing the competitive binding of the low affinity peptide H98 to trastuzumab. Rearrangement and elimination of variables resulted in the following cubic equation for *L1T*:

$$\begin{aligned} & a\ L1T^3 + b\ L1T^2 + c\ L1T + d = 0 \\ & a = K_{d2} - K_{d1} \\ & b = K_{d1}^{\ 2} - K_{d1}\ K_{d2} + K_{d1}\ L1_{tot} - 2K_{d2}\ L1_{tot} - K_{d1}\ L2_{tot} + K_{d1}\ T_{tot} - K_{d2}\ T_{tot} \\ & c = K_{d1}\ K_{d2}\ L1_{tot} + K_{d2}\ L1_{tot}^{\ 2} + K_{d1}\ L1_{tot}\ L2_{tot} - K_{d1}\ L1_{tot}\ T_{tot} + 2K_{d2}\ L1_{tot}\ T_{tot} \\ & d = -K_{d2}\ L1_{tot}^{\ 2}\ T_{tot} \end{aligned} \tag{S13}$$

Analytical solution for *L1T* and subsequent determination of the other four unknowns was performed using Mathematica (Wolfram Research, Champaign, IL), and the solution in which all roots were real was chosen. The MATLAB function, peptideAntibodyCompetition.m, calculating the solutions is available at https://github.com/pet90d/Fitting-of-ligand-competition.

Measurement of the dissociation of the trastuzumab-H98 complex using fluorescence anisotropy measurements

The binding of a small, fluorescently labeled ligand to a large binder results in a large, measurable increase in its fluorescence anisotropy based on which the dissociation constant

of the complex can be determined [3]. To this end, 1 μM dye-conjugated H98 was incubated with different concentrations of unlabeled or fluorescently-labeled trastuzumab followed by measuring the fluorescence anisotropy of the dye conjugated to H98. The fluorescent labels of the antibody and the antigenic peptide were chosen so that no or minimal FRET could take place between them. The following equation was fitted to the anisotropy data [4]:

$$r = \left(1 - \frac{c_{H98-trast}}{c_{tot,H98}}\right) r_{free} + \frac{c_{H98-trast}}{c_{tot,H98}} r_{bound} \qquad \text{(S14)}$$

where r is the anisotropy of the antibody-peptide mixture, r_{free} and r_{bound} are the anisotropies of the free and antibody-bound peptide, respectively, $c_{tot,H98}$ is the total concentration of the peptide, and $c_{H98\text{-}trast}$ is the concentration of the peptide-trastuzumab complex, which was calculated taking potential ligand depletion into account:

$$c_{H98-trast} = \frac{K_d + c_{tot,H98} + c_{tot,trast} - \sqrt{\left(K_d + c_{tot,H98}\right)^2 + 2\left(K_d - c_{tot,H98}\right)c_{tot,trast} + c_{tot,trast}^{\ 2}}}{2} \qquad \text{(S15)}$$

where $c_{tot,trast}$ is the total concentration of the antibody. Substitution of equation (S15) into equation (S14) resulted in an expression with three parameters to fit (K_d, r_{free}, r_{bound}). Fitting was performed with a custom-written program in Matlab (Mathworks, Natick, MA)

For the determination of the effect of glycerol on antibody affinity, the binding reaction was carried out in both water and in a 55% (v/v) aqueous solution of glycerol at 25°C. At this temperature, the dynamic viscosity of water is $8.93 \cdot 10^{-4}$ Pa s, while that of a 55% (v/v) aqueous solution of glycerol is $9.23 \cdot 10^{-3}$ Pa s (http://www.met.reading.ac.uk/~sws04cdw/viscosity_calc.html). In a certain solution (water or 55% glycerol), two curves were measured, the anisotropies of the unlabeled and the fluorescently-labeled antibodies. These two curves were fitted globally assuming that the maximum and minimum anisotropies of both curves are identical. The maximum anisotropy corresponds to saturated binding of H98 to the antibody, whereas the lowest anisotropy is the anisotropy of free H98. Using the known total concentrations of H98 and trastuzumab, the anisotropy was calculated according to equations (S14) and (S15), which involves the dissociation constant as a parameter. The global fitting algorithm, implemented in Matlab, minimized the squared deviation between the measured anisotropy values and those calculated using equations (S14) and (S15) resulting in the dissociation constant of the unlabeled and fluorescently-labeled trastuzumab. The Matlab

function performing the fitting, fitManyAniSatCurves.m, is available at https://github.com/pet90d/Fitting-of-ligand-competition.

Triple-FRET measurements

The triple-FRET measurements were performed according to a previously published method [5]. Intensities were measured in six different detection channels in which the intensities were determined by integrating the emission in certain spectral regions according to Fig. 2. The equation set describing the measured intensities is as follows:

$$
\begin{aligned}
I_1 &= I_A\left(1-E_{AB}-E_{AC}\right)\\
I_2 &= S_1\ I_A\left(1-E_{AB}-E_{AC}\right)+\alpha_{AB}\ I_A\ E_{AB}\left(1-E_{BC}\right)+S_4\ I_B\left(1-E_{BC}\right)\\
I_3 &= \alpha_{AC}\ I_A\left(E_{AB}\ E_{BC}+E_{AC}\right)+S_{12}\ \alpha_{AB}\ I_A\ E_{AB}\left(1-E_{BC}\right)+S_9\ I_A\left(1-E_{AB}-E_{AC}\right)+S_{10}\ I_B\left(1-E_{BC}\right)+S_7\ I_C\\
I_4 &= I_B\left(1-E_{BC}\right)\\
I_5 &= S_2\ I_B\left(1-E_{BC}\right)+\alpha_{BC}\ I_B\ E_{BC}+S_3\ I_C\\
I_6 &= I_C
\end{aligned}
\qquad \text{(S16)}
$$

Capital A, B and C in the subscripts refer to the fluorophores with A being the bluest, and C being the reddest. The parameters in the equation set are defined in the following table:

Parameter	Description
I_1	intensity excited at the absorption wavelength of A, detected in the emission range of A
I_2	intensity excited at the absorption wavelength of A, detected in the emission range of B
I_3	intensity excited at the absorption wavelength of A, detected in the emission range of C
I_4	intensity excited at the absorption wavelength of B, detected in the emission range of B
I_5	intensity excited at the absorption wavelength of B, detected in the emission range of C
I_6	intensity excited at the absorption wavelength of C, detected in the emission range of C
I_A	directly excited, unquenched intensity of A
I_B	directly excited, unquenched intensity of B
I_C	directly excited, unquenched intensity of C
E_{AB}	the FRET efficiency between A and B
E_{AC}	the FRET efficiency between A and C
E_{BC}	the FRET efficiency between B and C

The overspill parameters, *S*, were determined on samples labeled by a single kind of fluorophore and are defined by the following equations:

$$
\begin{aligned}
&S_1 = \frac{I_{A,2}}{I_{A,1}},\ S_9 = \frac{I_{A,3}}{I_{A,1}} \\
&S_2 = \frac{I_{B,5}}{I_{B,4}},\ S_4 = \frac{I_{B,2}}{I_{B,4}},\ S_{10} = \frac{I_{B,3}}{I_{B,4}},\ S_{12} = \frac{I_{B,3}}{I_{B,2}} \\
&S_3 = \frac{I_{C,5}}{I_{C,6}},\ S_7 = \frac{I_{C,3}}{I_{C,6}},
\end{aligned}
\tag{S17}
$$

where intensity $I_{Q,x}$ is the intensity of dye Q measured in detection channel x. The α parameters relating the detection efficiencies of different fluorophores in different detection channels to each other were determined according to the following equations:

$$
\begin{aligned}
\alpha_{AB} &= \frac{I_{B,2}}{I_{A,1}} \frac{c_A}{c_B} \frac{\varepsilon_{A,1}}{\varepsilon_{B,1}} \\
\alpha_{AC} &= \frac{I_{C,3}}{I_{A,1}} \frac{c_A}{c_C} \frac{\varepsilon_{A,1}}{\varepsilon_{C,1}} \\
\alpha_{BC} &= \frac{I_{C,5}}{I_{B,4}} \frac{c_B}{c_C} \frac{\varepsilon_{B,4}}{\varepsilon_{C,4}}
\end{aligned}
\tag{S18}
$$

where c is the molar concentration of the dye specified in the subscript, and $\varepsilon_{Q,x}$ is the molar absorption coefficient of dye Q at the excitation wavelength of detection channel x. The three FRET efficiencies can be calculated by solving equation set (S16) as follows:

$$
\begin{aligned}
E_{AB} &= \frac{\left(-I_2 + I_1\ S_1 + I_4\ S_4\right)\alpha_{AC}\left(I_5 - I_6\ S_3 + I_4\left(-S_2 + \alpha_{BC}\right)\right)}{I_4\left(\left(-I_3 + I_2\ S_{12} - I_1\ S_1\ S_{12} + I_4\left(S_{10} - S_{12}\ S_4\right) + I_6\ S_7 + I_1\ S_9\right)\alpha_{AB} + \left(-I_2 + I_4\ S_4 + I_1\left(S_1 - \alpha_{AB}\right)\right)\alpha_{AC}\right)\alpha_{BC}} \\
E_{BC} &= \frac{I_5 - I_4\ S_2 - I_6\ S_3}{I_5 - I_4\ S_2 - I_6\ S_3 + I_4\ \alpha_{BC}} \\
E_{AC} &= \frac{\left(I_5 - I_4\ S_2 - I_6\ S_3\right)\left(I_2 - I_1\ S_1 - I_4\ S_4\right)\alpha_{AC} + I_4\left(-I_3 + I_2\ S_{12} - I_1\ S_1\ S_{12} + I_4\left(S_{10} - S_{12}\ S_4\right) + I_6\ S_7 + I_1\ S_9\right)\alpha_{AB}\ \alpha_{BC}}{I_4\left(\left(-I_3 + I_2\ S_{12} - I_1\ S_1 S_{12} + I_4\left(S_{10} - S_{12}\ S_4\right) + I_6\ S_7 + I_1\ S_9\right)\alpha_{AB} + \left(-I_2 + I_4\ S_4 + I_1\left(S_1 - \alpha_{AB}\right)\right)\alpha_{AC}\right)\alpha_{BC}}
\end{aligned}
$$

(S19)

Determination of the extent of FRET due to a high concentration of free acceptors

If particles are randomly distributed in a 3D volume, the probability that the nearest neighbor of a certain particle is within FRET distance is a function of particle density. If FRET is measured between a donor on the antibody and an acceptor on the antigen, FRET can take place within the antibody-antigen complex, or between the antibody and free acceptors if the concentration of the latter is high enough so that random proximity may arise due to crowding effects. The probability that an acceptor is within FRET distance from a donor has to be determined to be able to estimate the probability of FRET due to random proximity. The

probability density of finding the k^{th} particle at distance r from a particle assuming complete spatial randomness in 3D is given by the following equation:

$$\mathrm{f}(r) = \frac{3}{(k-1)!}\ \lambda^k\ r^{3k-1}\ e^{-\lambda r^3} \tag{S20}$$

where

$$\lambda = \frac{\rho\ \pi^{3/2}}{\Gamma\left(\frac{3}{2}+1\right)} \tag{S21}$$

where Γ is the gamma function.

Integration of the former equation provides the cumulative distribution function, F(d):

$$\mathrm{F}(d) = \int_0^d \mathrm{f}(r)\,dr = \frac{d^{3k}\lambda^k\left(d^3\lambda\right)^{-k}\left(\Gamma(k) - \Gamma\left(k, d^3\lambda\right)\right)}{(-1+k)!} \tag{S22}$$

where Γ with two input parameters is the incomplete gamma function. The figure below shows the cumulative distribution function, F(d), for k=1 and λ calculated for a concentration of 3 μM, i.e., the probability that the first neighbor is found within a sphere of radius d. The concentration used was chosen to be 3 μM since the concentration of the acceptor-labeled antigenic peptide (H98) was 3 μM in the triple-FRET experiments.

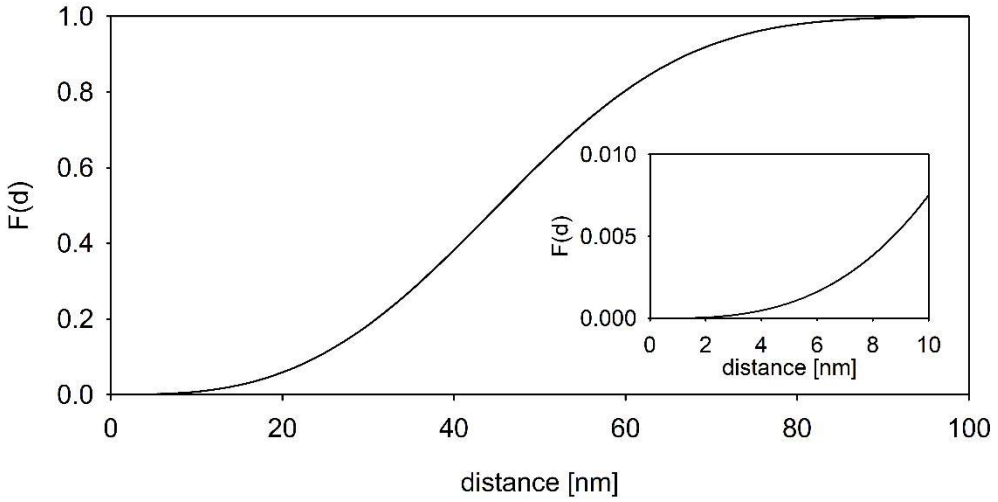

The graph, and in particular the insert, clearly shows that the probability of finding an acceptor-labeled peptide within 10 nm of a donor-labeled antibody is less than 0.01. Since FRET is practically impossible beyond a distance of 10 nm for the dyes used in the experiments, it can be concluded that free acceptors (free antigenic peptides) are unlikely to contribute to any significant extent to the measured FRET efficiencies, i.e., the FRET efficiency for the

process in which the acceptor is the antigenic peptide can be fully attributed to antibody-bound, acceptor-labeled antigens.

Supplementary Figures

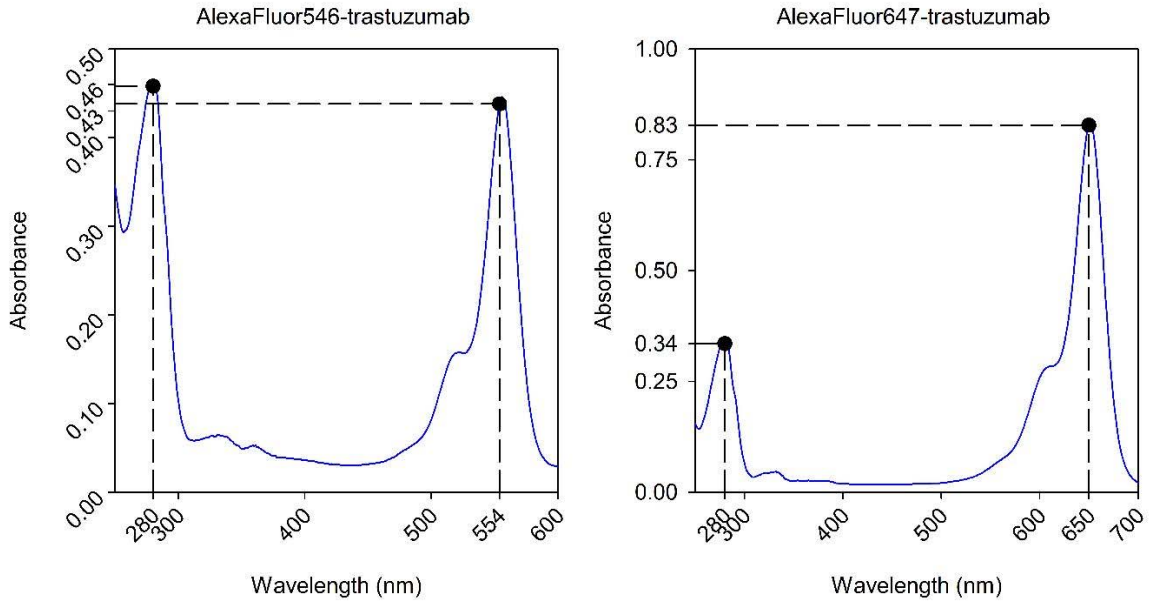

Supplementary Figure 1. Determination of the degree of labeling (DOL) using spectrophotometry. Absorption spectra of antibodies were recorded and the degree of labeling was calculated according the equations (S1)-(S6). The table below demonstrates the calculations step-by-step:

	AlexaFluor546-trastuzumab	AlexaFluor647-trastuzumab
peak absorption of dye	554 nm	650 nm
ε of dye at absorption peak	104,000 $M^{-1}cm^{-1}$	239,000 $M^{-1}cm^{-1}$
A(dye peak)	0.43	0.83
dilution factor	5	5
molar concentration of dye	20.7 μM	17.4 μM
ε of IgG at 280 nm	210,000 $M^{-1}cm^{-1}$	
CF	0.12	0.03
A(280)	0.46	0.34
molar concentration of IgG	9.7 μM	7.5 μM
DOL	2.1	2.3
concentration of IgG in mg/mL	1.46 mg/ml	1.13 mg/ml

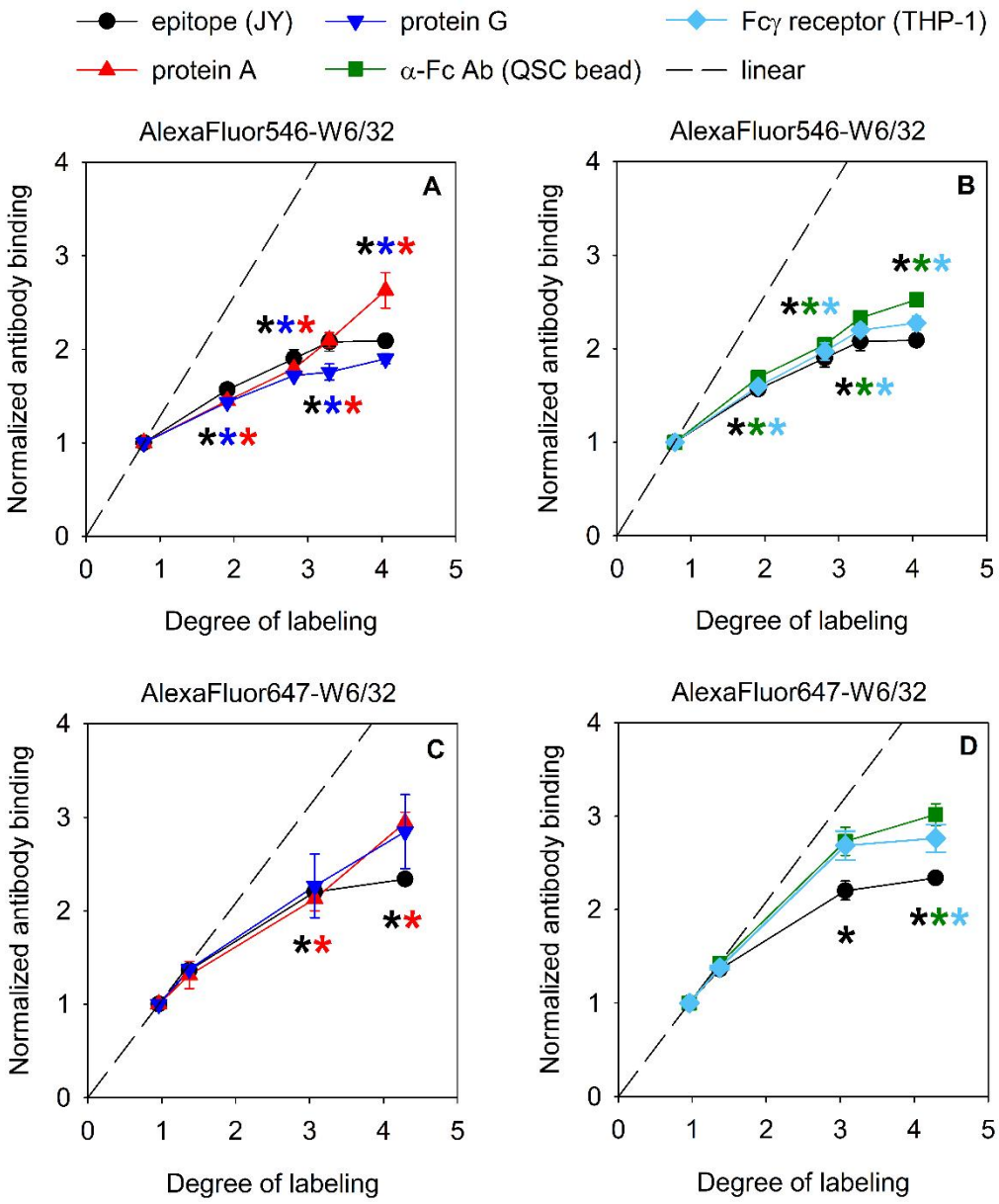

Supplementary Figure 2. Testing the functional properties of different domains of antibody W6/32 as a function of the degree of labeling. W6/32 was labeled either with AlexaFluor546 (A,B) or AlexaFluor647 (C,D) fluorophores. Antibody batches with 4-5 different degrees of labeling were generated, and their degree of labeling was determined by spectrophotometry. Epitope binding capability of the antibodies was tested by measuring their binding to JY cells expressing MHC-I, the antigen recognized by W6/32 (●). Their potential to bind to protein G or protein A was estimated by measuring their binding to protein G- (▼) or protein A-coated (▲) beads, respectively. The binding of W6/32 to Fcγ receptors was tested by measuring their binding to THP-1 cells expressing Fcγ receptors (◆) after blocking potential direct binding of W6/32 to cell surface-expressed MHC-I as described in Materials and Methods. The ability of W6/32 to be recognized by anti-mouse Fc receptor antibodies was tested by measuring their binding to anti-Fc antibody-coated QSC beads (■). In order to circumvent overcrowding of

figures, the binding of W6/32 to JY cells (●) is displayed in both the left- and right-hand figures, while binding to protein A and protein G (▲,▼) is only shown in the left-hand figures, and binding to Fcγ receptors and to anti-Fcγ receptor antibodies (◆,■) is only shown in the right-hand figures. Binding was measured by flow cytometry, and mean fluorescence intensities of flow cytometric histograms were normalized to the degree of labeling of the antibody batch with the lowest degree of labeling. This way of determining "normalized antibody binding", plotted on the vertical axis, results in a value of 1 for the antibody with the lowest degree of labeling. The dashed lines show how the normalized antibody binding would change if it were a linear function of the degree of labeling. The graphs show the means of three independent experiments (±the standard error of the mean). The asterisks indicate that the normalized antibody binding is significantly different from the linear expectation (the dashed line) that would be observed if the fluorescence intensity of the bound antibody fraction were proportional to the degree of labeling. One-sample t-tests were carried out at a level of significance of 5%, and a significant difference was concluded for $p<0.05$ adjusted for multiple comparisons according to Bonferroni. The color of the asterisks matches the color of the symbols.

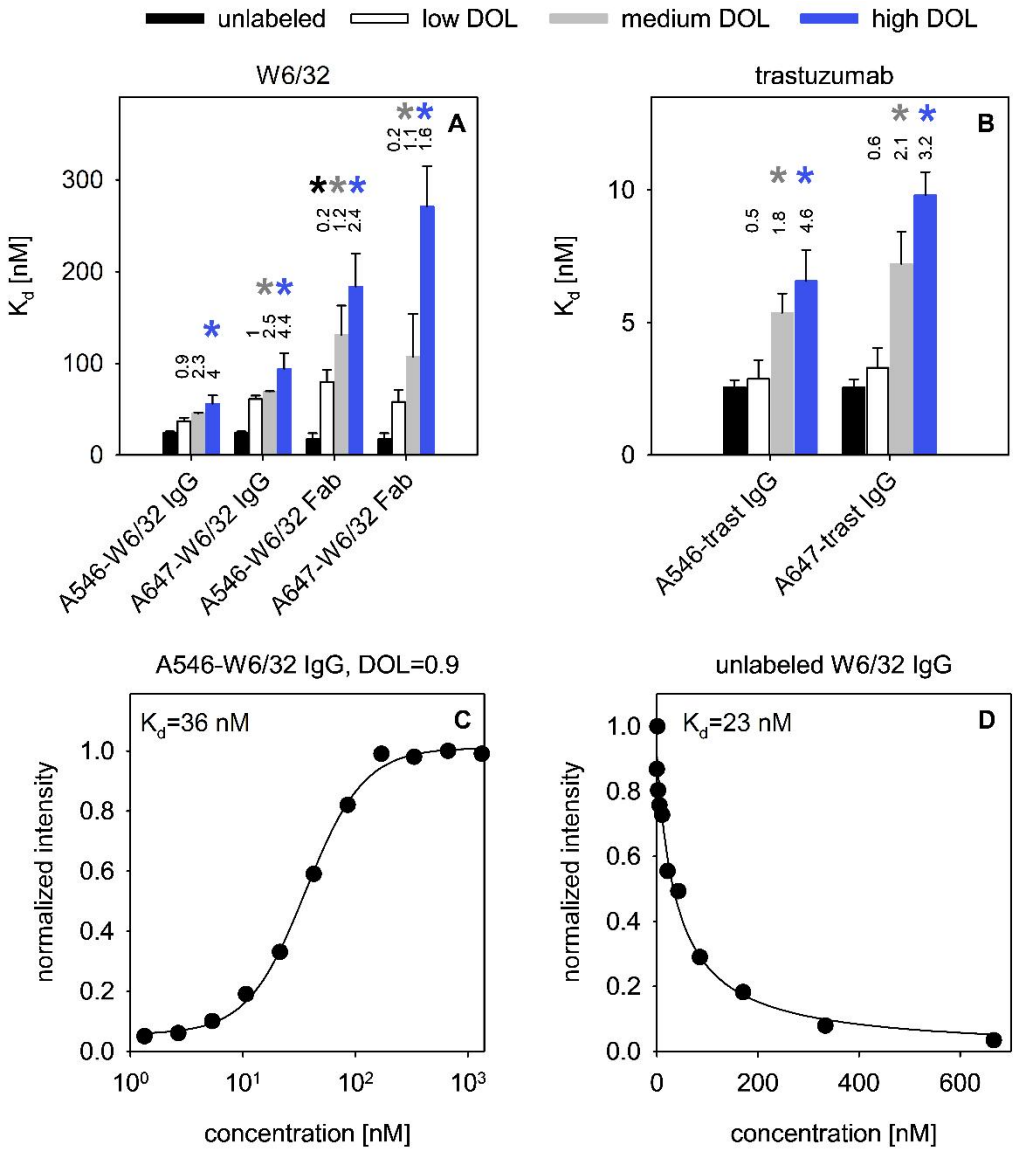

Supplementary Figure 3. Deterioration of IgG and Fab affinity as a function of the degree of labeling. W6/32 (A) and trastuzumab (B) IgG was labeled by AlexaFluor546 (A546 in the figure) or AlexaFluor647 (A647 in the figure) fluorophores. Fab fragments prepared from the W6/32 antibody were also labeled by either AlexaFluor546 or AlexaFluor647. The numbers above the bars show the degree of labeling determined by spectrophotometry. The dissociation constant (K_d) of the labeled antibodies was determined by measuring the fluorescence intensity of cell samples labeled by different concentrations of the IgG or Fab using flow cytometry followed by fitting a single site binding equation to the data. A representative curve of such a measurement is shown in C. The K_d of unlabeled antibodies and Fabs was determined by incubating cells with a constant concentration of a labeled antibody or Fab with a K_d determined previously and different concentrations of the unlabeled antibody or Fab of the same idiotype followed by fitting a competitive binding equation to the data. A representative curve from such an experiment is shown in D. The bars in parts A and B show the means of three independent experiments (±standard error of the mean). The asterisks indicate significant differences between K_d-s of the labeled and unlabeled antibodies (Dunnett's multiple comparisons test carried out after significant results in 2-way ANOVA, $p<0.05$).

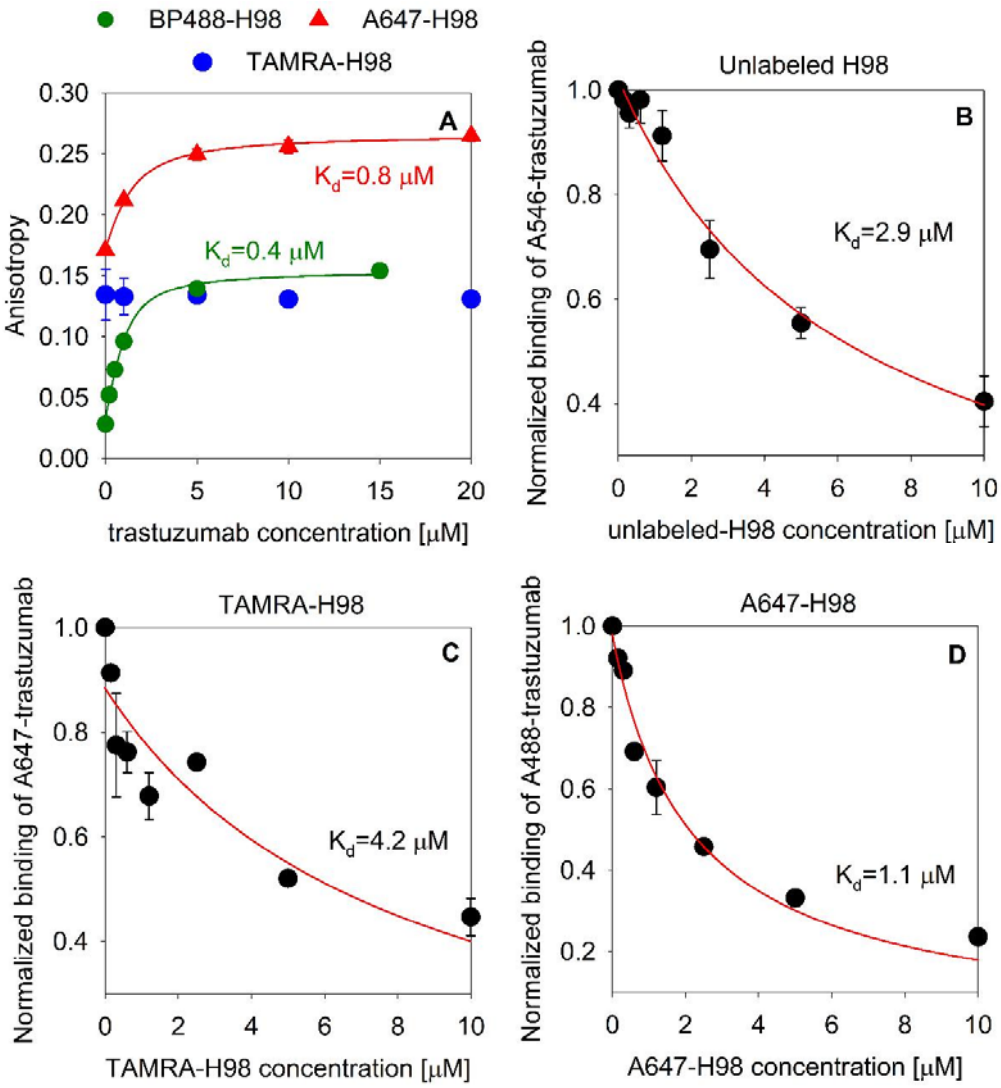

Supplementary Figure 4. Evaluation of the binding of H98 peptide to trastuzumab. (**A**) The binding of H98 labeled by either one of the three fluorophores (BP488, TAMRA or AlexaFluor647 designated A647 in the figure) to trastuzumab was studied by incubating 1 μM labeled H98 with the displayed concentrations of trastuzumab in solution followed by measuring the steady-state fluorescence anisotropy by fluorometry. A model described in section "Steady-state fluorescence anisotropy measurements" was fitted to the measurement data providing the dissociation constant of the H98-trastuzumab complex. The data of TAMRA-labeled H98 could not be evaluated due to the reported anomalous behavior of the anisotropy of TAMRA-conjugated compounds upon binding [6]. (**B-D**) Competitive binding of unlabeled H98 (B), TAMRA-H98 (C) and AlexaFluor647-H98 (D) to trastuzumab. SKBR-3 cells expressing ErbB2, the antigen recognized by trastuzumab, were incubated with a mixture containing 0.01 μM of fluorescently labeled trastuzumab and varying concentrations of H98 followed by washing and measurement of the fluorescence intensity of cell-bound trastuzumab by flow cytometry. The mean fluorescence intensity determined from three independent measurements was fitted according to the model described in section "Fitting a single site-two ligand model" in the Supplementary Materials using the known K_d of fluorescent trastuzumab as a constant parameter in the model providing the K_d of H98. The error bars in the figure represent the standard error of the mean (in many cases smaller than the symbols).

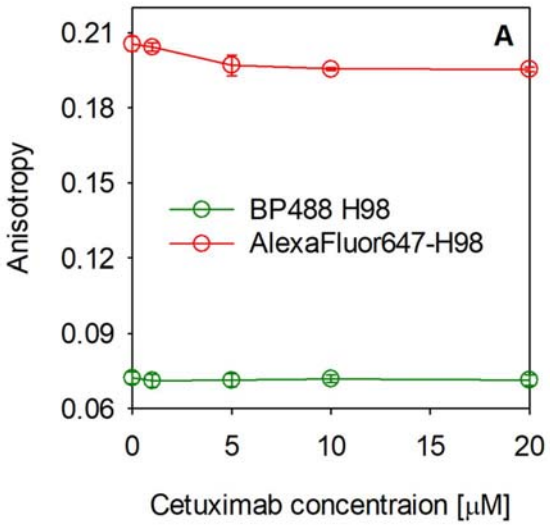

Supplementary Figure 5. Lack of nonspecific binding of H98 to trastuzumab. (**A**) The nonspecific binding of H98 labeled by either BP488 or AlexaFluor647 to cetuximab was studied by incubating 1 μM fluorescent H98 with the displayed concentrations of cetuximab in solution followed by measuring the steady-state fluorescence anisotropy by fluorometry. The error bars designate the standard error of the mean. TAMRA-H98 was not included in the experiments due to the anomalous behavior of TAMRA anisotropy shown in Suppl. Fig. 4A.

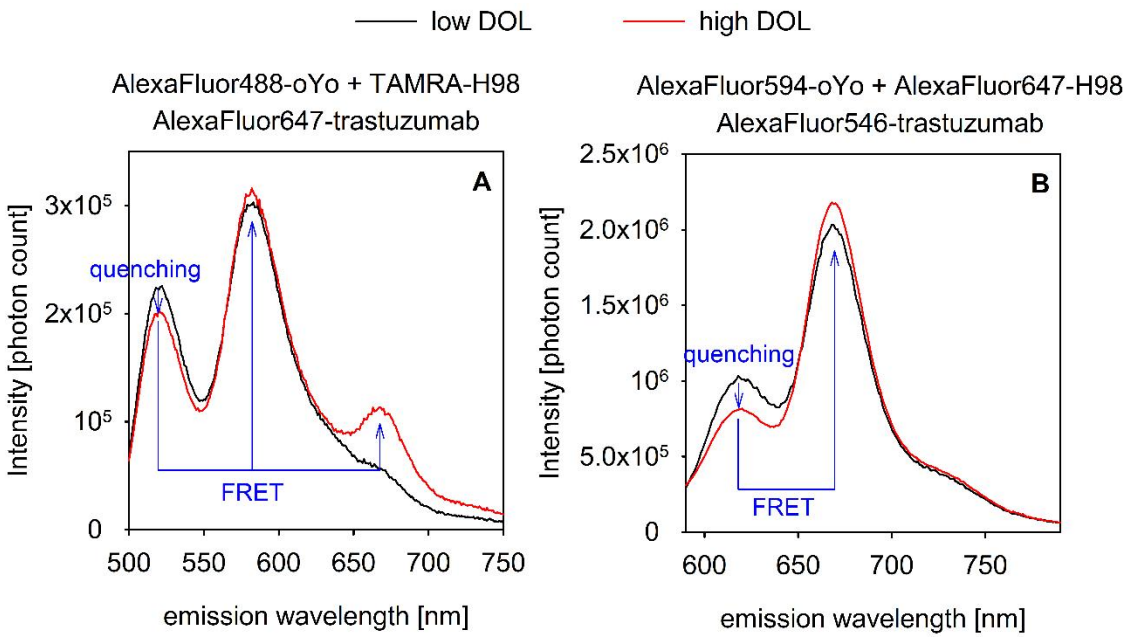

Supplementary Figure 6. Recording of FRET-sensitized emission spectra of triple-labeled antibody-antigen complexes. Trastuzumab was randomly labeled at lysine residues with AlexaFluor647 (A) or AlexaFluor546 (B) using conventional N-Hydroxysuccinimide ester chemistry. Antibodies with two different degrees of labeling (DOL) were generated for both dyes (low and high DOL for AlexaFluor647 are 0.8 and 3, respectively; low and high DOL for AlexaFluor546 are 1.5 and 3.4, respectively). The Fc portion of the antibodies was subsequently labeled with the oYo tag conjugated to AlexaFluor488 (A) or AlexaFluor594 (B). These dual-labeled antibodies were complexed with the H98 antigenic peptide conjugated with TAMRA (A) or AlexaFluor647 (B). This triple-FRET system depicted in Figure 2 was analyzed by exciting the complexes at the absorption wavelength of the dye attached to the oYo link (A: AlexaFluor488 was excited at 488 nm; B: AlexaFluor594 was excited 580 nm) and recording their emission spectra in the indicated wavelength range. The displayed spectra are uncorrected for spectral overspill. The blue arrows label those changes in the spectra that correspond to energy transfer from the dye in the oYo tag (on the Fc domain) to the epitope (in both panels A and B) and then further to the dyes on the antibody (only in panel A). Due to the large number of spectral overspills in the triple-FRET calculations, these changes can only be considered implications for the occurrence of FRET. Quantitative evaluation of the spectra by solving the triple-FRET equations is shown in Figure 3.

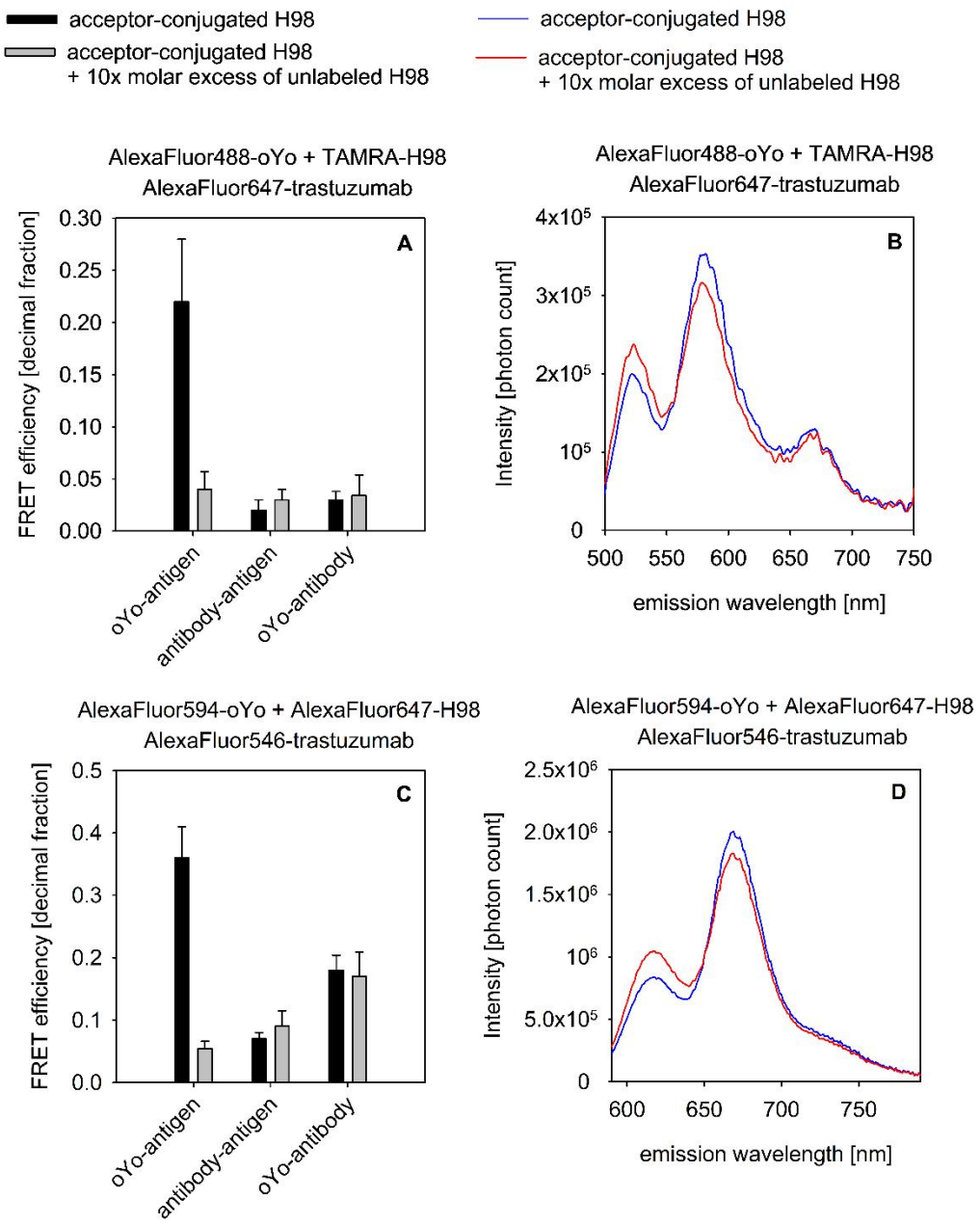

Supplementary Figure 7. Specific binding of the H98 antigenic peptide to trastuzumab in FRET experiments. AlexaFluor546-trastuzumab (C, D) and AlexaFluor647-trastuzumab (A, B) with a high degree of labeling (DOL=3.9 and DOL=4.9 for AlexaFluor546-trastuzumab and AlexaFluor647-trastuzumab, respectively) were incubated with their spectrally-matched, acceptor-conjugated H98 antigenic peptide in the absence or presence of a 10-fold molar excess of unlabeled H98. The conditions of the FRET measurements are identical to those described in Supplementary Figure 6 and Figure 3. Unquenching of the donor (the dye conjugated to the oYo-Link) and decreased sensitized emission of the acceptor on H98 in samples containing the 10-fold molar excess of unlabeled antigenic peptide show that acceptor-tagged H98 was displaced by unlabeled H98 (B, D). The calculated FRET efficiencies also corroborate these conclusions (A, C). The error bars in the bar graphs correspond to the standard error of the mean of three independent measurements.

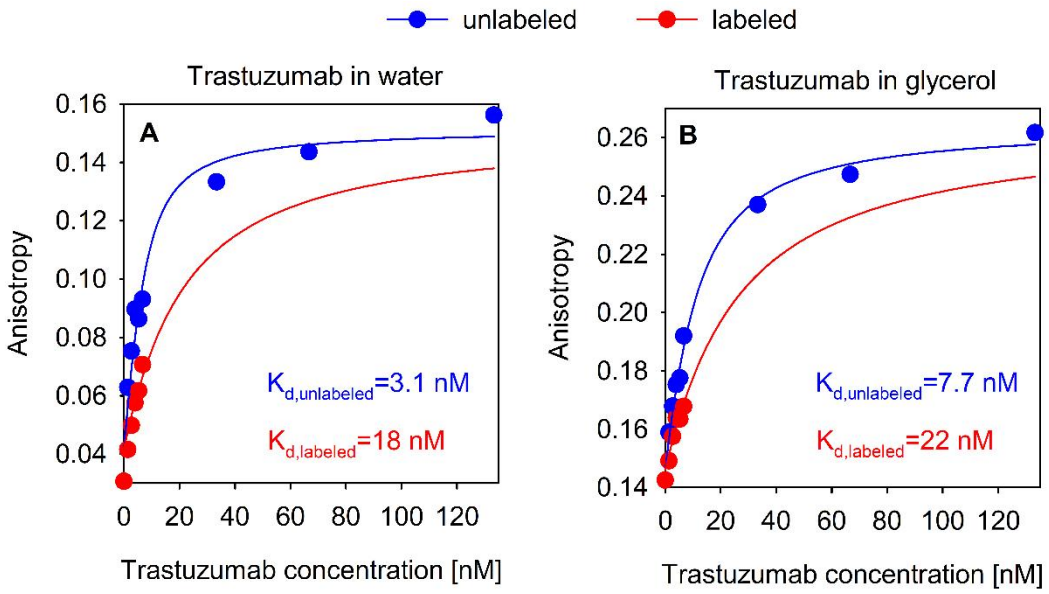

Supplementary Figure 8. Determination of the dissociation constant of the antibody-antigen complex in water and glycerol using fluorescence anisotropy measurements. The binding of unlabeled trastuzumab and AlexaFluor647-conjugated trastuzumab (DOL=3.7) to BP488-conjugated H98 in water (A) and 55% (v/v) glycerol (B) was investigated by measuring the fluorescence anisotropy of BP488 at 25°C. 1 µM of BP488-H98 was mixed with different concentrations of labeled or unlabeled trastuzumab either in water or in 55% (v/v) glycerol, and the fluorescence anisotropy of the BP488-labeled antigenic peptide (H98) was measured by fluorometry. The two graphs show a representative measurement in which the symbols correspond to the measured anisotropies, and the lines represent fits of the anisotropy model described in detail in section "Measurement of the dissociation of the trastuzumab-H98 complex using fluorescence anisotropy measurements" in the Supplementary Material. The displayed dissociation constants were determined by the fitting. As stated in the description of the fitting, the curves of the labeled and unlabeled antibodies were fitted globally assuming a common maximum anisotropy. This strategy enabled reliable estimation of the dissociation constant (K_d) for the labeled antibody as well, despite the limitation that its concentration could not be raised above ~10 nM due to the significantly lower concentration of the labeled stock relative to the unlabeled one.

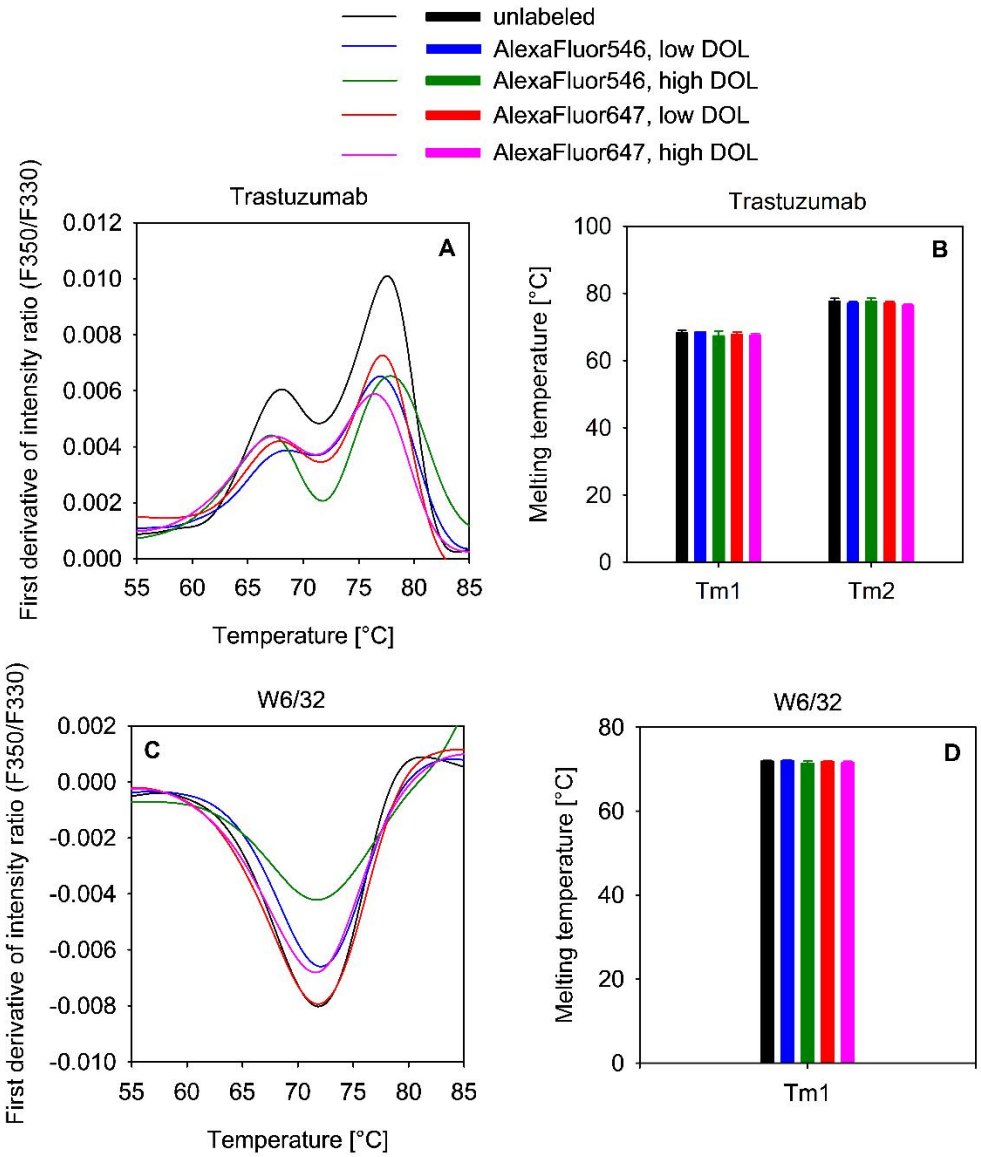

Supplementary Figure 9. Investigation of the thermal stability of IgG using nano differential scanning fluorometry. Trastuzumab and W6/32 were labeled with AlexaFluor546 or AlexaFluor647, and the degree of labeling (DOL) was determined by spectrophotometry. The degree of labeling of the investigated low-DOL and high-DOL antibodies is summarized in the table below:

	AlexaFluor546-labeled		AlexaFluor647-labeled	
	low-DOL	high-DOL	low-DOL	high-DOL
Trastuzumab	DOL=1.1	DOL=4.7	DOL=0.8	DOL=3.5
W6/32	DOL=1.9	DOL=3.6	DOL=1.4	DOL=3.3

The transition midpoint (melting temperature, T_m) was determined for both unlabeled and fluorescently labeled antibodies by measuring the emission ratio of endogenous tryptophane fluorescence at 350 and 330 nm (F350/F330) as a function of temperature. The first derivative of the intensity ratio is shown in panels A and C. The melting temperatures (±standard error of the mean) are shown in panels B and D.

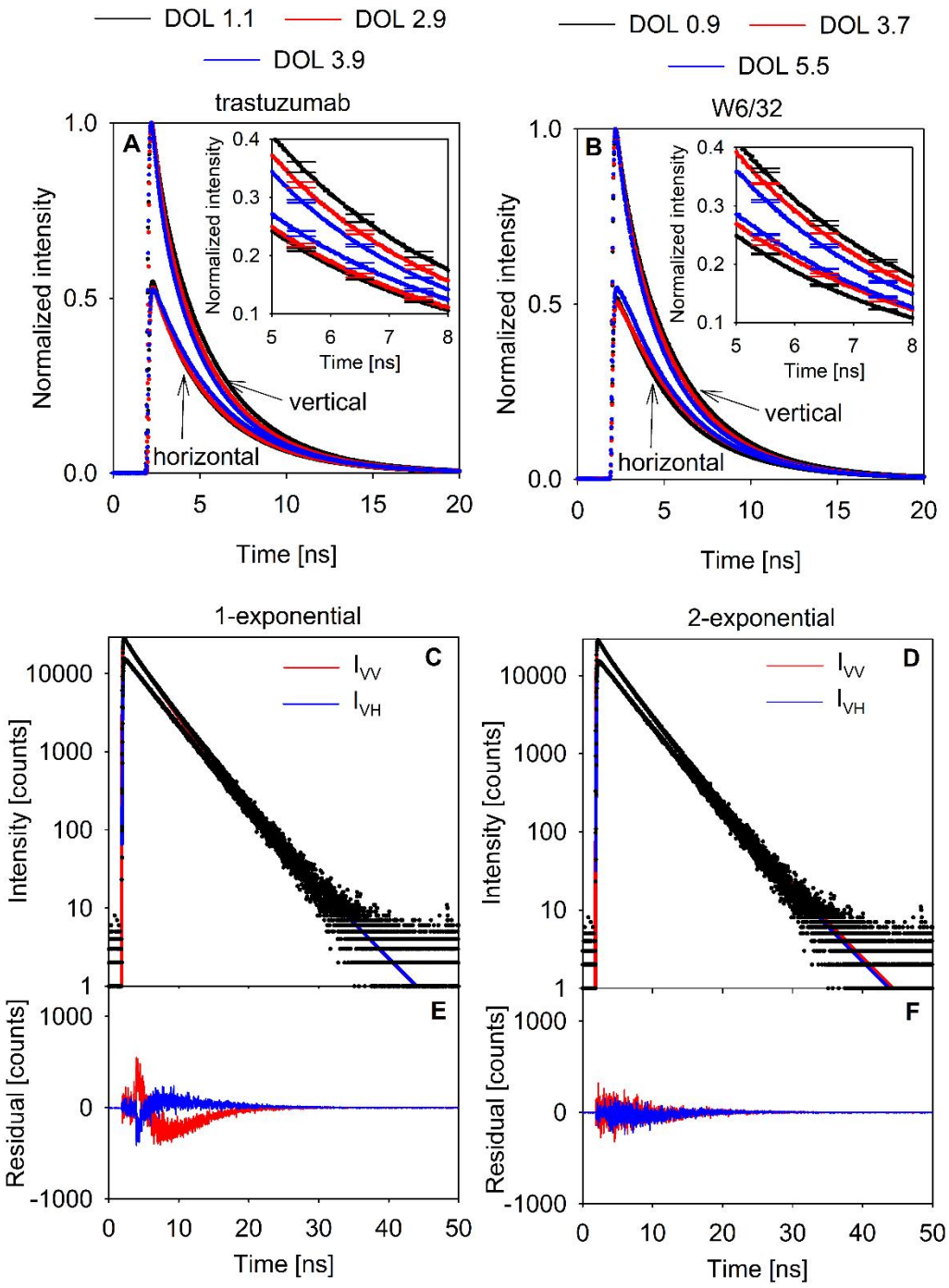

Supplementary Figure 10. Fluorescence anisotropy measurements and their analysis using reconvolution. Trastuzumab (A) or W6/32 (B) antibodies were labeled with AlexaFluor546 to achieve different degrees of labeling determined by spectrophotometry. The fluorescence anisotropy of AlexaFluor546 was measured by recording the vertical and horizontal components of their emission after pulsed, vertical excitation using time-correlated single photon counting. The normalized vertical and horizontal emission components are shown in A and B. The inserts showing the intensity traces between 5 and 8 ns and representative error bars (standard error of the mean) demonstrate that the decays of the vertical and horizontal intensity components are different beyond experimental error for the three antibodies with different degrees of labeling. Panels C-F show a representative evaluation of the time-dependent anisotropy decay of AlexaFluor546-trastuzumab (DOL=2.9). The vertical and horizontal intensity components were reconvolved with the instrument response function

assuming single-exponential (C) or double-exponential (D) anisotropy decays, and the anisotropy decay time constants were fitted. The fitted intensity decays are shown in panels C-D, and the residuals corresponding to the single- and double-exponential decays are shown in E and F.

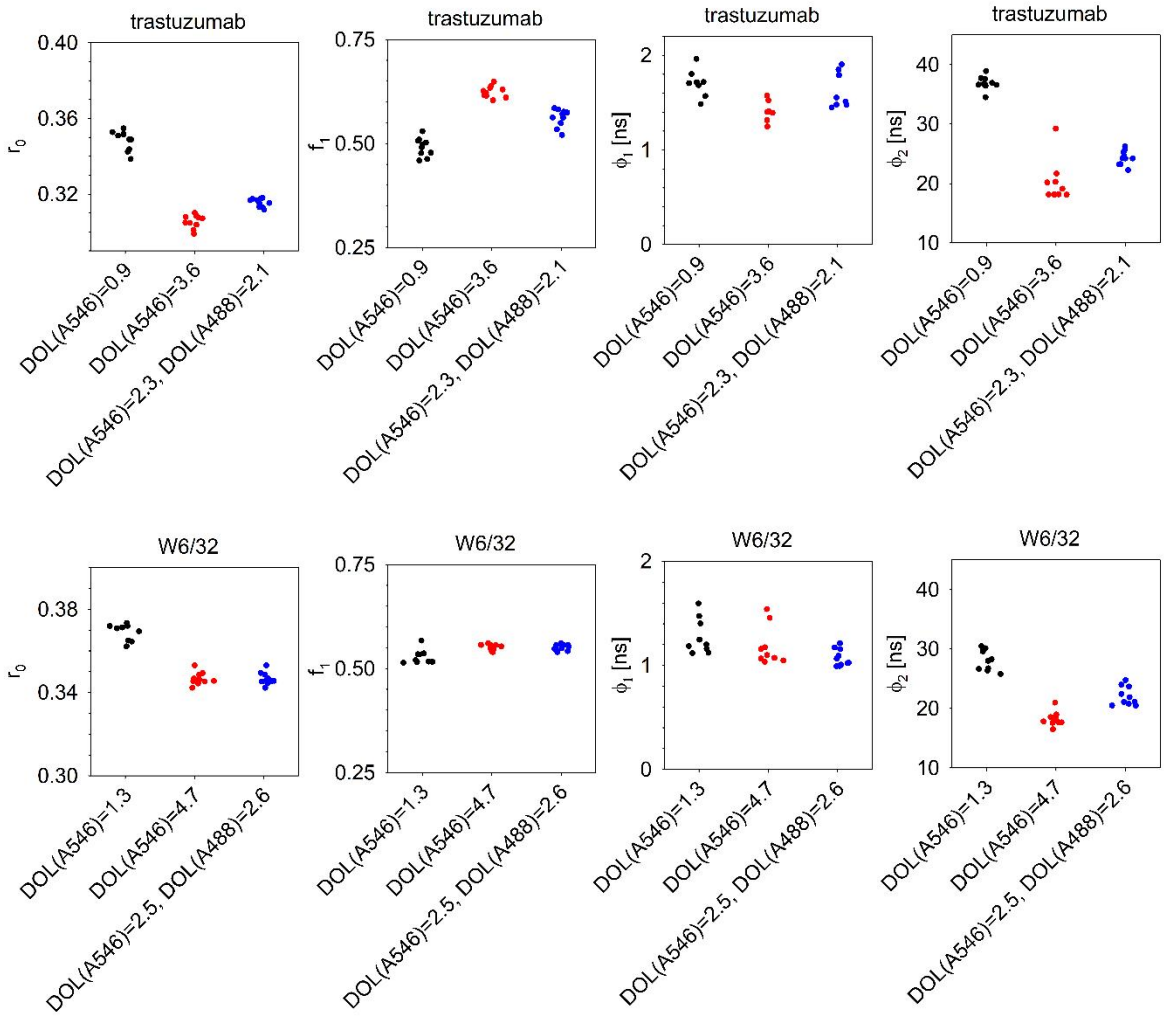

Supplementary Figure 11. Analysis of the fluorescence anisotropy decay of single- and double-labeled antibodies. Trastuzumab and W6/32 antibodies were either single-labeled by AlexaFluor546 (A546), or double-labeled with both AlexaFluor546 and AlexaFluor488 (A488), and their degrees of labeling (DOL) were determined by spectrophotometry. Time-dependent fluorescence anisotropy decay curves were recorded by time-correlated single photon counting followed by analysis of the anisotropy decay parameters using a reconvolution approach. The maximum anisotropy (r_0), the fraction of the first anisotropy decay component (f_1) and the anisotropy decay time constants of the first and second components (φ_1, φ_2) of individual measurements are shown in the figure.

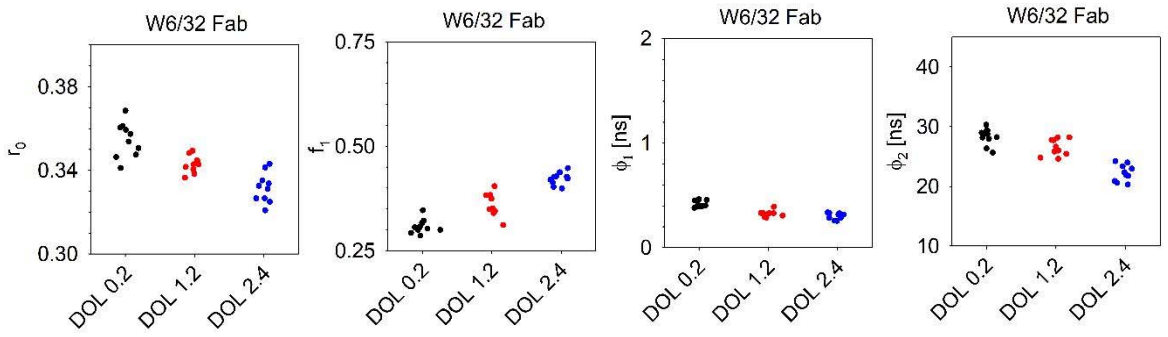

Supplementary Figure 12. Investigation of the time-dependent decay of fluorescence anisotropy of fluorescently-labeled Fab fragments. Fab fragments prepared from the W6/32 antibody were labeled by AlexaFluor546, and the degree of labeling (DOL) was determined by spectrophotometry. Time-dependent fluorescence anisotropy decay curves were recorded by time-correlated single photon counting followed by analysis of the anisotropy decay parameters using a reconvolution approach. The maximum anisotropy (r_0), the fraction of the first anisotropy decay component (f_1) and the anisotropy decay time constants of the first and second components (φ_1, φ_2) of individual measurements are shown in the figure.

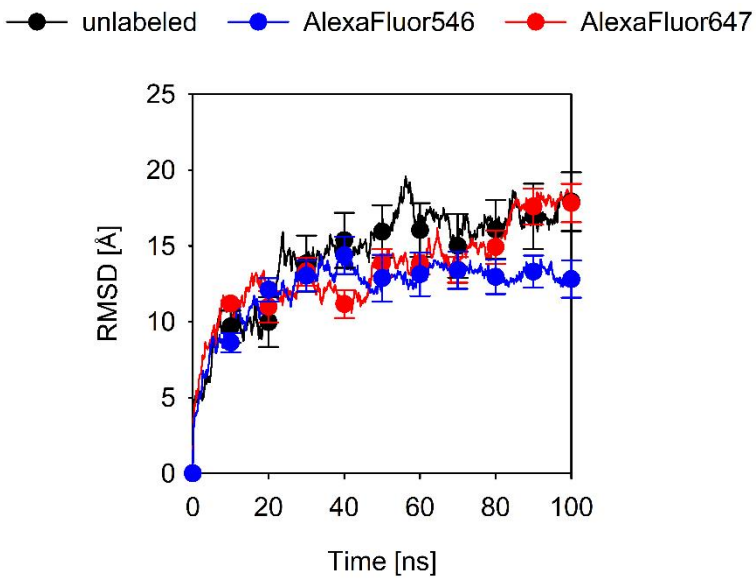

Supplementary Figure 13. Root mean square deviation (RMSD) of simulated trastuzumab structures. The RMSD of C_α atoms was calculated for the whole structure of unlabeled and fluorescently labeled trastuzumab, and it is plotted alongside the standard error of the mean of every 100th data point calculated from the four MD simulations as a function of simulation time.

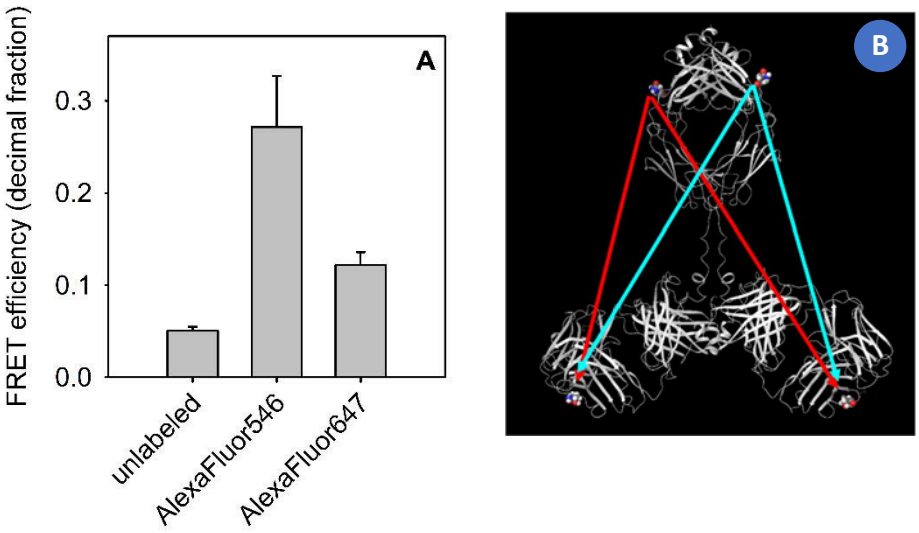

Supplementary Figure 14. Determination of the FRET efficiency between the epitope binding site and the Fc portion of trastuzumab from molecular dynamics simulations. MD simulations of unlabeled, AlexaFluor546-conjugated and AlexaFluor647-conjugated trastuzumab were performed using four random initiations of velocities for all three antibody versions. Thr58 in the heavy chain is located in the epitope binding region of trastuzumab [7]. Asn437 of the heavy chain is within the region binding to protein G from which the Fc-specific oYo-Link was engineered [8, 9]. These amino acids are shown using ball representation in the ribbon representation of trastuzumab (panel B). Since the Fc part was labeled by the donor and the acceptor was present in the antigen, a donor can undergo FRET to either one of the acceptors (shown by the arrows in panel B). The donor-acceptor distance for these two FRET processes was calculated in the last 30 ns of the MD simulations, and it was averaged for the two FRET processes. The expected FRET efficiency from the Fc portion to the epitope binding site was calculated according to the following equation:

$$E = \frac{R_0^{\,6}\left(R_1^{\,6} + R_2^{\,6}\right)}{R_1^{\,6}\,R_2^{\,6} + R_0^{\,6}\left(R_1^{\,6} + R_2^{\,6}\right)}$$

that takes into account the two independent FRET processes from the donor, labeling the Fc part, to the epitope labeled by the acceptor. In the formula, R_1 and R_2 are the distances from the donor in the Fc domain to the two acceptors in the epitope binding region, and R_0 is the Förster radius of the donor-acceptor pair ($R_{0,\,\text{A488-TAMRA}}$=6.37 nm, used for the AlexaFluor647-conjugated antibody; $R_{0,\,\text{A594-A647}}$=7.7 nm, used for the AlexaFluor546-conjugated antibody; see Figure 2 for details of the fluorescence labeling strategy). The plotted FRET values are the averages for the two donors present in the Fc part. These expected FRET efficiencies along with their standard error of the mean values are shown in panel A.

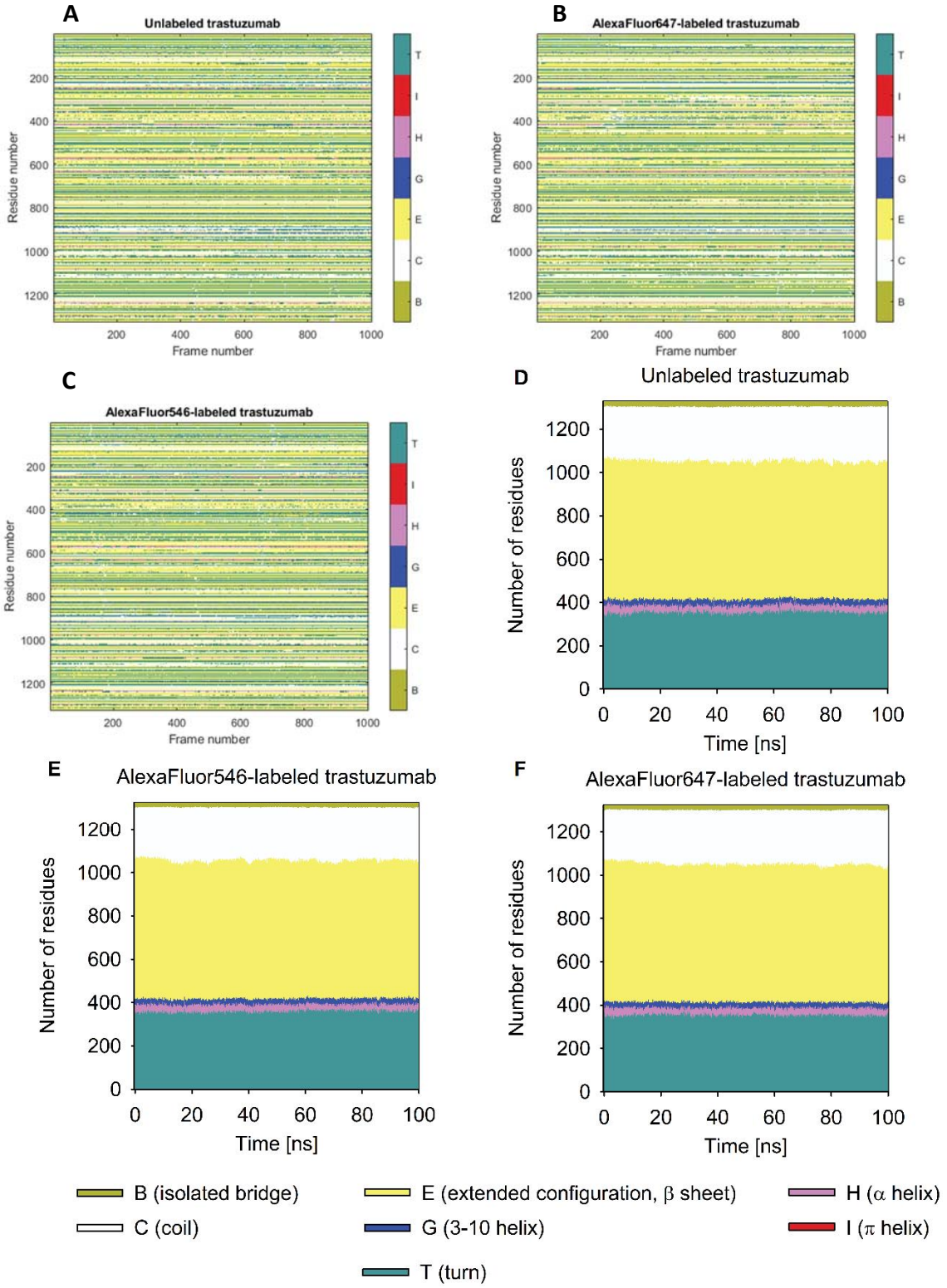

Supplementary Figure 15. Analysis of the secondary structure of unlabeled and labeled trastuzumab in MD trajectories. The secondary structure composition of unlabeled and fluorescently labeled trastuzumab was analyzed based on the MD simulation trajectories using VMD. Panels A-C show the secondary structure assignment of every residue in each frame of a representative simulation. Meaning of the single letter codes is shown at the bottom of the figure. Panels D-F show the fraction of residues residing in certain kinds of secondary structure elements calculated as the average of the four MD simulations.

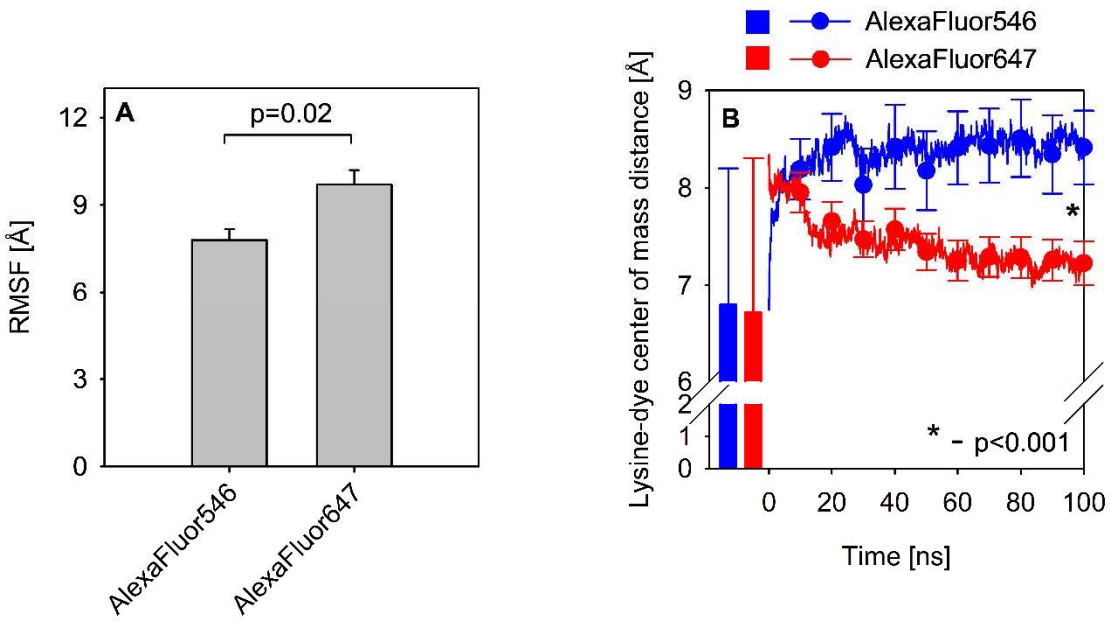

Supplementary Figure 16. Analysis of the dynamics of antibody-conjugated AlexaFluor dyes. **A**. The average root mean square fluctuation (RMSF) of all the antibody-conjugated AlexaFluor546 or AlexaFluor647 molecules was determined, and they are shown along with the standard deviation calculated for all the dyes in the four MD simulations. The RMSF of the two dyes was compared with a two-sample t-test and found to be significantly different (p=0.02). **B**. The center of mass of the antibody-conjugated fluorophores was calculated, and its distance from the ε-amino nitrogen of the labeled lysines was determined and averaged for all the dyes coupled to the antibody in all four MD simulations. The line graph shows the mean distances for the two different kinds of fluorophores. The error bars, shown for every 100th time point in the trajectory, correspond to the standard error of the mean. The two bars display the same distances for the free dyes simulated under the same conditions. The asterisk indicates a significant difference between the values of the two dyes calculated using a two-sample t-test for the last time point.

Supplementary Tables

Supplementary Table 1. Absorption and emission maxima of the dyes used in the experiments

Dye	**Absorption maximum [nm]**	**Emission maximum [nm]**
AlexaFluor488, BP488	495	520
TAMRA	552	578
AlexaFluor546	556	573
AlexaFluor594	590	617
AlexaFluor647	650	668

Supplementary Table 2. The effect of glycerol on the dissociation constant of the H98-trastuzumab complex. The errors correspond to the standard error of the mean.

antigen	antibody	dissociation constant [μM]	
		aqueous medium	55% (v/v) glycerol
AlexaFluor647-H98	unlabeled trastuzumab	0.92±0.15	1.54±0.24
	AlexaFluor546-trastuzumab (degree of labeling=3.5)	2.12±0.22	2.14±0.23
BP488-H98	unlabeled trastuzumab	0.45±0.01	1.28±0.08
	AlexaFluor647-trastuzumab (degree of labeling=4.6)	3.59±0.43	3.88±0.33

References

[1] C. O'Fagain, P.M. Cummins, B.F. O'Connor, Gel-Filtration Chromatography, Methods Mol Biol 1485 (2017) 15-25.

[2] Alexa Fluor Dyes Spanning the Visible and Infrared Spectrum. https://www.thermofisher.com/hu/en/home/references/molecular-probes-the-handbook/fluorophores-and-their-amine-reactive-derivatives/alexa-fluor-dyes-spanning-the-visible-and-infrared-spectrum.html.

[3] A. Gijsbers, T. Nishigaki, N. Sanchez-Puig, Fluorescence Anisotropy as a Tool to Study Protein-protein Interactions, J Vis Exp (116) (2016).

[4] D.M. Jameson, J.A. Ross, Fluorescence polarization/anisotropy in diagnostics and imaging, Chem Rev 110(5) (2010) 2685-708.

[5] A. Fábián, G. Horváth, G. Vámosi, G. Vereb, J. Szöllősi, TripleFRET measurements in flow cytometry, Cytometry A 83(4) (2013) 375-85.

[6] J.C. Stern, B.J. Anderson, T.J. Owens, J.F. Schildbach, Energetics of the sequence-specific binding of single-stranded DNA by the F factor relaxase domain, J Biol Chem 279(28) (2004) 29155-9.

[7] O. Olaleye, C. Graf, B. Spanov, N. Govorukhina, M.R. Groves, N.C. van de Merbel, R. Bischoff, Determination of Binding Sites on Trastuzumab and Pertuzumab to Selective Affimers Using Hydrogen-Deuterium Exchange Mass Spectrometry, J Am Soc Mass Spectrom 34(4) (2023) 775-783.

[8] A.E. Sauer-Eriksson, G.J. Kleywegt, M. Uhlen, T.A. Jones, Crystal structure of the C2 fragment of streptococcal protein G in complex with the Fc domain of human IgG, Structure 3(3) (1995) 265-78.

[9] J.Z. Hui, S. Tamsen, Y. Song, A. Tsourkas, LASIC: Light Activated Site-Specific Conjugation of Native IgGs, Bioconjug Chem 26(8) (2015) 1456-60.